Cluster dynamical mean-field theories: Causality and classical limit

G. Biroli,[1] O. Parcollet,[1] and G. Kotliar[2]
[1]*Service de Physique Theorique, CEA Saclay, 91191 Gif-Sur-Yvette, France*
[2]*Center for Materials Theory, Department of Physics and Astronomy, Rutgers University, Piscataway, New Jersey 08854, USA*
(Received 30 July 2003; published 28 May 2004)

Cluster dynamical mean field theories are analyzed in terms of their semiclassical limit and their causality properties, and a translation invariant formulation of the cellular dynamical mean-field theory, periodized cluster dynamical mean-field theory (PCDMFT), is presented. The semiclassical limit of the cluster methods is analyzed by applying them to the Falikov-Kimball model in the limit of infinite Hubbard interaction U where they map to different classical cluster schemes for the Ising model. Furthermore, the Cutkosky-t'Hooft-Veltman cutting equations are generalized and derived for nontranslation invariant systems using the Schwinger-Keldysh formalism. This provides a general setting to discuss causality properties of cluster methods. To illustrate the method, we prove that PCDMFT is causal while the nested cluster schemes in general and the pair scheme in particular are not. Constraints on further extension of these schemes are discussed.

DOI: 10.1103/PhysRevB.69.205108 PACS number(s): 71.10.−w, 71.30.+h

I. INTRODUCTION

Dynamical mean field theory (DMFT) (for a review see Ref. 1) has been very successful in providing a nonperturbative approach to strongly correlated Fermi systems. It describes both the localized and the itinerant limit and has yielded nonperturbative insights into the finite-temperature Mott transition.[1] This approach has been combined with realistic electronic structure methods such as local-density approximation and GW and has been applied successfully to numerous materials.[2] In spite of these successes, several limitations of the single-site DMFT approach are now apparent. For example, the self-energy is k independent by construction, so the method cannot describe independent variations of the quasiparticle residue, the quasiparticle lifetime, and the effective mass. Furthermore, the single-site nature of the method precludes it from treating more exotic orders with order parameters involving several sites, such as dimerization, staggered flux or d-density wave, and d-wave superconductivity.

To overcome these limitations, various extensions of DMFT have been proposed. For a disordered system, one can set up a functional integral formulation, with DMFT as a saddle point, leading to a natural loop expansion.[3] A formulation of these ideas for a clean system is still lacking. A different extension is the extended DMFT (EDMFT),[4] in which the DMFT ansatz is applied simultaneously to bosonic and fermionic degrees of freedom. This approach does not describe a k-dependent self-energy but incorporates diagrams involving longer-range interactions into the DMFT equations.

A different idea is based on truncations of the Baym-Kadanoff functional. In the full theory, this is a functional of the full Green functions. DMFT is obtained by restricting it to local Green functions only, setting the nonlocal Green functions equal to zero. A natural extension is to restrict the functional to local and nearest-neighbor Green functions. This pair scheme was introduced independently by Ingersent and Schiller,[5] and by Georges and Kotliar.[1] The latter authors observed noncausal behavior in an iterated perturbation theory solution of the Hubbard model, but the origin of this problem was not elucidated. Zarand *et al.* suggested[6] that the pair cluster approach was causal, and that the difficulties encountered in the solution were related to the impurity solver rather than to the scheme itself, but no conclusive proof of this statement was presented. This pair method requires a simultaneous solution of multiple-site impurity problems.

A different direction was pursued by Jarrell and collaborators with the introduction of dynamical cluster approximation (DCA),[7] whose main idea is to discretize uniformly momentum space. This approach was shown to be manifestly causal. It can also be formulated in real space[8] (see also Appendix A). A different approach, the cellular DMFT or CDMFT, motivated by applications to electronic structure, was introduced in Ref. 9. In this approach, the many-body problem is truncated by introducing a finite basis set of orbitals to truncate the self-energy. It introduces the cluster self-energy and the lattice self-energy as independent entities. This method was tested in a soluble model,[8] in the Falikov-Kimball model,[10] and in the one-dimensional Hubbard model.[11] These papers developed the CDMFT ideas from a real-space perspective. In this paper we develop this approach from a momentum-space perspective, to maintain periodicity in the self-consistency equation. The importance of including this periodicity was underlined by Lichtenstein,[12,13] arguing that the lack of periodicity of CDMFT could unfavor phases, like the d-wave superconductivity, in which the order parameter lives on links. Even though this point has not yet been elucidated, it is certainly desirable to have a generalization of CDMFT that is translation invariant and causal in its use of the lattice self-energy in the self-consistency condition.

Cluster DMFT methods have not yet reached the level of understanding of their single-site counterparts. While the single-site DMFT can be unambiguously formulated, cluster DMFT methods are more diverse and therefore require more detailed methodological investigation, since the virtues and

limitations of the various cluster schemes are not apparent yet. This paper is a contribution in this direction.

There are several important principles that a cluster method should satisfy.

(i) Given that cluster DMFT approximations are intrinsically basis dependent, a cluster method should be formulated in a general basis set. This flexibility is important, because for a given problem, one could carry out the cluster DMFT study in the basis which is most suitable for the system in question.

(ii) It should have an effective action formulation, namely, it should target the calculation of a specific correlator function.

(iii) It should yield causal Green functions.

(iv) It should be able to capture the various orders, including those which break the translation invariance.

(v) It should converge rapidly as a function of the discretization parameter for the observable that one is targeting. It is possible that different cluster schemes may converge better for different observables. A better understanding of these elements of a cluster method is desirable.

In Sec. II, we present our translation invariant generalization of CDMFT where the lattice self-energy participates in the self-consistent equation. This is a different cluster scheme, and we formulate it in a way which allows a comparison with CDMFT and DCA. We also discuss in Sec. II C a different class of schemes, the *nested cluster schemes*, which require the simultaneous consistent solutions of impurity models of different size.

In Sec. III, in an attempt to clarify the nature of the various cluster approximations, we study their classical limit in the Ising limit of the Falikov-Kimball model. The various schemes then reduce to classical cluster approximations to the Ising model. This analysis elucidates their physical content at the classical level and it allows a simple and clear comparison. This study complements other comparisons of cluster schemes against more exact treatments for specific models.[8,10] The classical limit of EDMFT was discussed in Ref. 14.

In Sec. IV, we analyze the issue of causality of cluster methods from a diagrammatic perspective using the Cutkovsky-t'Hooft-Veltman rules. We rederive them for non-translation invariant cases using the Schwinger-Keldysh formalism. We end up with a general setting to analyze the causality of cluster schemes. Within this framework we show that the pair scheme is not causal, and elucidate the origin of the problem. Furthermore, we provide a simple proof of the causality of CDMFT and DCA (which had already been proved by other methods) and justify the causality of the periodic generalization of CDMFT. Finally we make a relationship with the earlier paper of Mills *et al.* on disordered systems:[15] in fact, the coherent potential approximation (CPA) is a particular case of a DMFT. The origin of violations of causality and their possible cure for the generalizations of CPA were clarified by Mills.[15]

II. DESCRIPTION OF THE CLUSTER METHODS

A fairly general model of strongly correlated electrons contains hopping and interaction terms. It is defined on a lattice of $\mathcal{N}$ sites in d dimensions, and we divide the lattice in $(\mathcal{N}/L)^d$ cubic clusters of $S_c=L^d$ sites (more general forms can also be considered). We denote with $\mathbf{r}_\mu$ the internal cluster position and with $\mathbf{R}_n$ the cluster position in the lattice (therefore the position of the μth site of the nth cluster is R_n+r_μ). The lattice Hamiltonian is expressed in terms of fermionic operators $c^\dagger_{R_n,\alpha,\sigma}$ and $c_{R_m,\beta,\sigma}$ and can be written as

$$H=\sum_{n,\alpha,m,\beta,\sigma} t_{\alpha,\beta}(R_n-R_m)c^\dagger_{R_n,\alpha,\sigma}c_{R_m,\beta,\sigma} + \sum_{n,\alpha,\sigma_1,m,\beta,\sigma_2,n',\alpha',\sigma_3,m',\beta',\sigma_4} U_{\alpha,\sigma_1,\beta,\sigma_2,\alpha',\sigma_3,\beta',\sigma_4}(\{R\})c^\dagger_{R_n,\alpha,\sigma_1}c_{R_m,\beta,\sigma_2}c^\dagger_{R_{n'},\alpha',\sigma_3}c_{R_{m'},\beta',\sigma_4}, \quad (1)$$

where σ is an internal degree of freedom (i.e., a spin, spin orbital, or band index). Note that throughout this paper, we will denote the position and momentum on the (original) lattice with lowercase letters (r and k), the position and momentum of the superlattice with uppercase letters (R and K), and with greek letters α, β, γ, δ, μ, ν, ρ, λ the position within the cluster. Different dynamical cluster methods for strongly correlated electrons have been introduced in order to obtain an approximate solution of Eq. (1) able to capture the effect of short-range (dynamical) correlation and to describe the self-energy k dependence.

In the following, we introduce a scheme, the periodized cluster dynamical mean-field theory (PCDMFT), formulate CDMFT and DCA in real and k space and the *nested cluster schemes* (NCS), i.e., the pair scheme and its generalizations. CDMFT (Ref. 9) is a real-space cluster: the lattice is divided in a superlattice of cells and the scheme is basically the DMFT equations on the superlattice.[1] On the other hand, DCA (Ref. 7) is a reciprocal space cluster, where the self-energy in momentum space is approximated by step function around a few points, which we will denote by K_c and are identified to the momentum of the (periodic) cluster. We will show that PCDMFT is a natural generalization of both schemes, from a real-space and a k-space perspective.

A. Real-space perspective

Cluster methods for strongly correlated electrons (CDMFT, DCA, PCDMFT) can be divided in two steps. (Nested cluster schemes will be considered separately.)

The first step is the computation of the local cluster propagator $G_{c\mu\sigma_1\nu\sigma_2}(\tau)$ and the cluster self-energy Σ^{C} from an effective action containing a Weiss dynamical field $G^{-1}_{0,\mu\sigma_1\nu\sigma_2}(\tau,\tau')$ and the intracluster interaction:

$$S_{\mathrm{eff}}=-\int\int_0^\beta d\tau d\tau' c^\dagger_{\mu,\sigma_1}(\tau)G^{-1}_{0,\mu,\sigma_1,\nu,\sigma_2}(\tau,\tau')c_{\nu,\sigma_2}(\tau') + \int_0^\beta d\tau U_{\alpha,\sigma_1,\beta,\sigma_2,\gamma,\sigma_3,\delta,\sigma_4}(R=0) \times(c^\dagger_{\alpha,\sigma_1}c_{\beta,\sigma_2}c^\dagger_{\gamma,\sigma_3}c_{\delta,\sigma_4})(\tau), \tag{2a}$$

$$G_{c\mu,\sigma_1,\nu,\sigma_2}(\tau)=-\langle Tc_{\mu,\sigma_1}(\tau)c^\dagger_{\nu,\sigma_2}(0)\rangle_{S_{\mathrm{eff}}}, \tag{2b}$$

$$\Sigma^{\mathrm{C}}=G_0^{-1}-G_c^{-1}. \tag{2c}$$

In the following, we will often concentrate on square clusters of linear size L on a d-dimensional square lattice, although many of the results can be generalized easily. Hence, μ,ν will also denote the position of the cluster sites on the lattice: $\mu,\nu\in\mathcal{C}=\{0,\ldots,L-1\}^d$ where the intersite distance is normalized to 1. We will denote by S_c the cluster's size and by $\mathcal{C}$ the set of cluster points; σ is the spin index as mentioned earlier. In the following, we will consider only solutions with diagonal propagators in the internal index σ and for simplicity each time quantities are diagonal in the internal index σ we will omit it.

The second step consists in recomputing the Weiss field using the value of the self-energy obtained by the first step and then iterating until convergence is reached. The real difference between cluster schemes is how the second step is performed. We first focus on translational invariant cases. CDMFT is a direct generalization of DMFT to a cluster *in real space* and consists simply in rewriting the DMFT equations in a matrix form (μ,ν indices are omitted) taking as elementary degrees of freedom all the cluster fermionic degrees of freedom:

$$G_0^{-1}(i\omega_n)=\left(\sum_{K\in\mathrm{R.B.Z.}}\frac{1}{i\omega_n+\mu-\hat{t}(K)-\Sigma^{\mathrm{C}}(i\omega_n)}\right)^{-1}+\Sigma^{\mathrm{C}}(i\omega_n), \tag{3}$$

where $\hat{t}_{\mu\nu}(K)$ is the hopping expressed in the superlattice notations, with K in the reduced Brillouin zone (R.B.Z.) of the superlattice [see Eq. (A1)]. Note that from now on the sum over K means always the normalized sum. When convergence is reached and the cluster self-energy has been obtained, the translation invariant lattice self-energy $\Sigma^{\mathrm{latt}}[(i,j)$ denotes a site on the original lattice] is computed by the formula

$$\Sigma^{\mathrm{latt}}_{i-j}(\omega)=\frac{1}{S_c}\sum_{\substack{\mu,\nu\in\mathcal{C}\\ \mu-\nu=i-j}}\Sigma^{\mathrm{C}}_{\mu\nu}(\omega). \tag{4}$$

Other estimators (which still preserve causality) have been introduced in Ref. 8. Note that in CDMFT, the cluster and the lattice self-energy are two different quantities:[9] one has to first solve the cluster problem, and only at the end compute the lattice self-energy Σ^{latt}. In CDMFT, Σ^{latt} does not enter the self-consistency condition.

DCA is more naturally formulated in Fourier space.[7] However, it can also be recovered from a real-space perspective[8] just changing the hopping matrix in Eq. (3) to (see also Appendix A):

$$\hat{t}^{\mathrm{DCA}}_{\mu\nu}(K)\equiv t_{\mu\nu}(K)\exp[-iK(\mu-\nu)].$$

In this case if the self-energy is a cyclic matrix (translation invariant within the cluster) then Eq. (3) reduces to (upon diagonalization)

$$G_0^{-1}(K_c,i\omega_n)=\left(\sum_{K\in\mathrm{R.B.Z.}}\frac{1}{i\omega_n+\mu-t(K+K_c)-\Sigma^{\mathrm{C}}(K_c,i\omega_n)}\right)^{-1}+\Sigma^{\mathrm{C}}(K_c,i\omega_n), \tag{5}$$

which is the standard DCA equation introduced in Ref. 7 where $t(K)$ is the Fourier transform on the R.B.Z. of the hopping on the original lattice. Note that if the self-energy is cyclic then the Weiss field computed by Eq. (5) will be cyclic, so this property is preserved within the self-consistent loop. In DCA, contrary to CDMFT, there is no distinction between the cluster and the lattice self-energy. Because it is formulated in k space, DCA is also naturally translation invariant.

We are now ready to define the scheme PCDMFT for periodized CDMFT. The simplest definition is to take Σ^{latt} in place of Σ^{C} in the self-consistency condition. This is very close to the scheme proposed by Lichtenstein and Katsnelson in Ref. 13, with the big difference that PCDMFT is causal, as will be proved below. Thus the equations relating the self-energy to the Weiss field are

$$\Sigma_{\mathrm{latt}}(k,i\omega_n)=\frac{1}{S_c}\sum_{\mu,\nu\in\mathcal{C}}\Sigma^{\mathrm{C}}_{\mu\nu}(i\omega_n)\exp[-ik(\mu-\nu)], \tag{6a}$$

$$G_{\mu\nu}=\sum_k\frac{e^{-ik\cdot\mu}e^{ik\cdot\nu}}{i\omega_n+\mu-t(k)-\Sigma^{\mathrm{latt}}(k,i\omega_n)}, \tag{6b}$$

$$G_0^{-1}=G^{-1}+\Sigma^{\mathrm{C}}, \tag{6c}$$

where k is in the Brillouin zone of the original lattice.

The three schemes (CDMFT, DCA, PCDMFT) can be summarized into the same matrix equations: Eq. (2a) and

$$G_0^{-1}(i\omega_n)=\left(\sum_{K\in \mathrm{R.B.Z.}}[i\omega_n+\mu-\hat{t}_S(K)-\Sigma_S(K,i\omega_n)]^{-1}\right)^{-1}+\Sigma^{\mathrm{C}}(i\omega_n), \tag{7}$$

where the difference between the three schemes is enclosed in the value of t_S and of Σ_S that enter in the self-consistency condition.

Let us now turn to translation invariance breaking phases, where translation invariance is conserved on the superlattice (e.g., antiferromagnet, charge density, ''stripes'' if the cluster is big enough). CDMFT can describe such an order by construction since it does not require the translation invariance. When solved numerically (e.g., with quantum Monte Carlo method), the translation invariant solutions are often found to be instable towards the ordered one (we have explicitly encountered this phenomenon, for example, for antiferromagnetism and charge-density wave).

DCA and PCDMFT require translation invariance, therefore they need to be generalized to handle such an order. For DCA there are two solutions for this problem, for example, for antiferromagnetic order: (i) keep a reciprocal space formulation with a reduced Brillouin zone and introduce some correlation between k and $k+Q$, with $Q=(\pi,\pi)$;[16] (ii) use the *real-space formulation* introduced in Ref. 8, where translation invariance in the cluster *can* be broken, and look for an antiferromagnetic solution. It is shown in Appendix A that the two approaches are equivalent. However, (i) requires to anticipate the appearance of ordered phase, i.e., to adapt the cluster scheme for the order to be described: one needs to use a special setup for antiferromagnetic order, another for a more complicated order, whereas (ii) does not require to anticipate the order: it will show up automatically solving the real-space DCA equations with no need to generalize the scheme (provided that the cluster is big enough to contain the unit cell). The same numerical code will produce a translation invariant solution or an antiferromagnetic one, a stripelike one. In particular, since translation invariant solutions are often found to be numerically instable, one cannot miss an ordered phase with this approach. Therefore, the *real-space formulation* of DCA is the best solution from a practical point of view.

The PCDMFT is unfortunately more complicated to generalize. In the following, we will focus on square clusters on the square lattice. It is useful to introduce a slightly more general formula for Σ^{latt} for a bipartite lattice. The lattice self-energy is a sum of the cluster self-energy put at all possible positions on the lattice. We can rewrite Eq. (4) in a more transparent way, as a sum over all possible shifts of the cluster:

$$\Sigma^{\mathrm{latt}}_{\sigma,\mu;\sigma',\nu}(K)=\frac{1}{S_c}\sum_{\delta\in\{0,\ldots,L-1\}^d} e^{-iK(\lfloor(\mu+\delta)/L\rfloor-\lfloor(\nu+\delta)/L\rfloor)L}\times\Sigma^{\mathrm{C}}_{\sigma,\overline{\mu+\delta};\sigma',\overline{\nu+\delta}}, \tag{8}$$

where $\lfloor x\rfloor$ is the integer defined by $\lfloor x\rfloor\leqslant x<\lfloor x\rfloor+1$ (for a vector it has to be understood component by component), d is the dimension, δ is a d-dimensional shift vector, the bar denotes the modulo reduction by L component by component (adding δ is a circular shift in the cluster).

The idea of the generalization is then simple. In a phase that breaks translation invariance (we take antiferromagnet as an example), we have multiple solutions (two for AF), denoted by an index α ($\alpha=1,2$ for AF). In order to respect the order, we need to compensate the shift in the cluster by the change of solution: in the AF example, use one solution on one sublattice, another on the other sublattice. The formula is then

$$\Sigma^{\mathrm{latt}}_{\sigma,\mu;\sigma',\nu}(K)=\frac{1}{S_c}\sum_{\delta\in\{0,\ldots,L-1\}^d} e^{-iK(\lfloor(\mu+\delta)/L\rfloor-\lfloor(\nu+\delta)/L\rfloor)L}\times\Sigma^{\mathrm{C}\alpha(\delta)}_{\sigma,\overline{\mu+\delta};\sigma',\overline{\nu+\delta}}, \tag{9a}$$

$$\alpha(\delta)=\begin{cases}1 & \text{if} \quad \sum_{i=0}^{d}\delta_i=0 \ [2]\\ 2 & \text{if} \quad \sum_{i=0}^{d}\delta_i=1 \ [2].\end{cases} \tag{9b}$$

For the AF phase and when the original model is SU(2) invariant, the solution $\alpha=2$ is simply obtain from $\alpha=1$ by a spin flip. This does not need to be true in general, either for more complicated order or the Falikov-Kimball model that we will use in Sec. III. Let us note, however, that this generalization is more complex than for the DCA scheme from a practical perspective: the expression of Σ^{latt} strongly depends on the order to be described and on the form of the cluster.

B. Reciprocal space perspective: Φ derivation

We now explore the relation between PCDMFT, CDMFT, and DCA from the reciprocal space perspective. In order to do this, we use the generating functional formulation of DMFT.[1] Let us recall that one can define a functional $\Gamma(G)$,

$$\Gamma(G)=\mathrm{Tr}\ln G-\mathrm{Tr}\,G_0^{-1}G+\Phi(G), \tag{10}$$

where $G_0=(i\omega_n-t+\mu)^{-1}$ is the bare propagator and $\Phi(G)$, the Baym-Kadanoff functional, is the sum of all the vacuum two-particle irreducible diagrams constructed with the propagator G and the interaction vertices. The solution of the stationarity equation (11) is the real propagator of the full interacting theory. DMFT, as well as its cluster generalizations, can be seen as an approximation onto $\Phi(G)$. Indeed one obtains the DMFT approximation restricting $\Phi(G)$ only to single-site propagator (equating to zero all the non-single-site propagators), i.e., $\Phi_{\mathrm{DMFT}}(G)=\Sigma_i\Phi(G_{ii}|G_{ij}=0)$ or, equivalently, neglecting the momentum conservation at the vertices. These two procedures, which are equivalent at the single-site level, represent two different routes in order to obtain cluster generalization of DMFT.

CDMFT can be obtained by a natural real-space extension of the DMFT approximation on Φ:

$$\Phi_{\mathrm{CDMFT}}(G)=\sum_R \Phi(G_{\mu,R;\nu,R}|G_{\rho,R;\lambda R'}=0). \tag{11}$$

It is easy to show that the stationarity equation corresponding to this choice of Φ gives back the CDMFT equations. Note that the summation of the infinite series of diagram of $\Phi_{\mathrm{CDMFT}}(G)$ is performed by the cluster impurity solver like in the DMFT case.

DCA is formulated more naturally as an approximation in Fourier space: instead of neglecting completely the momentum vertex conservation one puts a coarse-grained δ inside the complete diagrammatic series.

$$\Phi_{\mathrm{DCA}}(G)=N_{ss}\Phi(G(k))|_{U(k_1,k_2,k_3,k_4)=U_{\mathrm{DCA}}(k_1,k_2,k_3,k_4)}, \tag{12}$$

where

$$U_{\mathrm{DCA}}(k_1,k_2,k_3,k_4)=\delta_{K_c(k_1)+K_c(k_2),K_c(k_3)+K_c(k_4)}/N_{ss},$$

N_{ss} is the number of clusters (number of sites divided by number of sites per cluster) and $K_c(k)$ is a function that for each k gives the center of the $[\pi/L,\pi/L]^d$ cube to which k belongs.[7]

PCDMFT has been introduced previously from the real-space point of view like a natural generalization of CDMFT in which one puts the lattice self-energy inside the self-consistent loop (still preserving the causality properties of CDMFT). In the following we shall show that, from the functional point of view, PCDMFT can also be seen at the same time as a translation invariant formulation of CDMFT and as a generalization of DCA. Up to now we restricted the discussion to the standard completely localized basis set for simplicity. However, CDMFT and PCDMFT can be formulated in a general basis set. This flexibility is important, because for a given problem, one could carry out the analysis in the basis which is most suitable for the system in question. As a consequence, in the following we will derive PCDMFT for a general basis.

We shall show that there are two different procedures leading to the same formulation of PCDMFT. Let us focus first on the one which shows that PCDMFT is the natural translation invariant formulation of CDMFT. Call $\varphi_{R\alpha}$ the basis function used to define the cellular DMFT (Ref. 9) and $\tilde{\varphi}_{R\alpha}$ their Fourier transform. Note that they are normalized in such a way that $\Sigma_i|\varphi_{R\alpha}(i)|^2=1,\Sigma_k|\tilde{\varphi}_{R\alpha}(k)|^2=1$. The particular case of the standard completely localized basis set corresponds to $\tilde{\varphi}_{R\alpha}(k)=\exp(-ikx_{R\alpha})/\sqrt{N}$ (N is the total number of sites) where $x_{R\alpha}=R+r_\alpha$. CDMFT in a general basis is obtained (i) keeping only the intracluster interaction, $U_{R_1\alpha,R_2\beta,R_3\gamma,R_4\delta}\rightarrow U_{R\alpha,R\beta,R\gamma,R\delta}$, and (ii) making the approximation (11) discussed above to the Baym-Kadanoff functional.

PCDMFT can be obtained making the approximations (i), (ii) and *imposing* the translational invariance of the original problem. This is performed expressing the propagator in the new basis set in terms of the translational invariant propagator in the original basis set:

$$G_{R\alpha,R'\beta}(\omega)=\sum_k \tilde{\varphi}_{R\alpha}(k)^*\hat{G}(k,\omega)\tilde{\varphi}_{R'\beta}(k). \tag{13}$$

Plugging this expression inside the functional leading to CDMFT, we get the PCDMFT functional

$$\Gamma(\hat{G}(k))=\mathrm{Tr}\ln(\hat{G})+\mathrm{Tr}\{[i\omega_n-t(k)+\mu]\hat{G}\}+N_{ss}\Phi_{\mathrm{PCDMFT}}(\tilde{U},\hat{G}), \tag{14}$$

where Φ is the Baym-Kadanoff functional expressed in terms of $\hat{G}(k)$ and obtained replacing the original matrix of interactions $U(k_1,k_2,k_3,k_4)$ with

$$\tilde{U}(k_1,k_2,k_3,k_4)=\sum_{\alpha,\beta,\gamma,\delta}U_{0\alpha,0\beta,0\gamma,0\delta}\tilde{\varphi}_{0\alpha}(k_1)\tilde{\varphi}^*_{0\beta}(k_2)\times\tilde{\varphi}_{0\gamma}(k_3)\tilde{\varphi}^*_{0\delta}(k_4), \tag{15}$$

where we made use explicitly of the translation invariance to put $R=0$.

Extremizing this functional with respect to $\hat{G}(k)$ gives the PCDMFT equations together with the form of the lattice self-energy:

$$G_{R\alpha,R\beta}(\omega)=\sum_k \tilde{\varphi}^*_{R\alpha}(k)\frac{1}{\omega-t(k)-\Sigma_{\mathrm{latt}}(k,\omega)}\tilde{\varphi}_{R\beta}(k), \tag{16a}$$

$$\Sigma_{\mathrm{latt}}(k,\omega)=\sum_{\alpha\beta R}\tilde{\varphi}^*_{R\alpha}(k)\Sigma^c_{\alpha\beta}\tilde{\varphi}_{R\beta}(k), \tag{16b}$$

where $\Sigma^c_{\alpha\beta}$ is the self-energy obtained from a cluster impurity problem characterized by a propagator $G^c_{\alpha,\beta}=G_{R\alpha,R\beta}$ and the interaction matrix $\tilde{U}_{\alpha\beta\gamma\delta}$.

As discussed before, there is another procedure to get the functional formulation of PCDMFT encoded in Eq. (14). As the DMFT approximation can be obtained just by neglecting the momentum conservation at the vertex, one can interpret Eq. (15) as an improvement to the DMFT approximation in which the vertex is replaced by $\tilde{U}(k_1,k_2,k_3,k_4)=\Sigma_{\alpha,\beta,\gamma,\delta}\tilde{U}_{\alpha,\beta,\gamma,\delta}\tilde{\varphi}_{0\alpha}(k_1)\tilde{\varphi}_{0\beta}(k_2)\tilde{\varphi}_{0\gamma}(k_3)\tilde{\varphi}_{0\delta}(k_4)$ where $\tilde{U}_{\alpha,\beta,\gamma,\delta}=U_{0\alpha,0\beta,0\gamma,0\delta}$.

At this point a natural question is why we have chosen this particular $\tilde{U}$ and, more interestingly, could other choices lead to a better approximation and what is the procedure to find the "best" $\tilde{U}$? Unfortunately we do not have clear answers to these questions. A partial answer to the first one is that the choice of $\tilde{U}$ leading to PCDMFT is the one that we obtain applying the least square minimization to $U(k_1,k_2,k_3,k_4)-\tilde{U}(k_1,k_2,k_3,k_4)$. So in a certain sense it provides the best approximation to U within the chosen basis set. It is, however, important to notice that it is far from clear that this is a good criterion to select the "best" $\tilde{U}$. With respect to these remarks, it is particularly interesting to note that DCA can be obtained taking $\tilde{U}_{\alpha,\beta,\gamma,\delta}=U_{0\alpha,0\alpha,0\alpha,0\alpha}\delta_{\alpha,\beta}\delta_{\gamma,\delta}\delta_{\delta,\gamma}$ (in the case of a complete diagonal interaction on the original lattice) and $\tilde{\varphi}_{R\beta}(k)=\exp[-iK_c(k)x_{R\beta}]/\sqrt{N}$.[7]

This suggests interesting interpolation between DCA and PCDMFT. A particularly simple one consists in dividing the Brillouin zone in l^d squares (like in DCA for a cluster of linear size l) and taking $\tilde{\varphi}_{R\mu}(k)=\exp[-iF_l(k)x_{R\mu}]/\sqrt{N}$ where $F_l(k)$ is a function giving, for each k, the center of the $[\pi/l,\pi/l]^d$ cube to which k belongs (note that $\mu=1,\ldots,L_c$). When $l=L_c$ one gets DCA, whereas when $l=\infty$ one gets PCDMFT.

Let us finally note that this functional derivation of PCDMFT is crucial to prove simply its causality properties. Indeed this scheme is causal because it is a composition of two causal steps. Clearly, starting from a causal cluster self-energy, one obtains a causal cluster propagator through Eqs. (16a) and (16b). Furthermore, we will show in Sec. IV that plugging the causal cluster propagator inside the diagrammatic series corresponding to the PCDMFT functional gives a causal cluster self-energy.

C. Nested cluster schemes

Another natural generalization of DMFT to the cluster setting is to apply the ideas connected to the cluster variation method (CVM) of classical statistical mechanics to the Baym-Kadanoff functional.[17,18] These schemes are also natural generalizations of the n site CPA (Ref. 19) to interacting electrons. The approach is defined by selecting a set of maximal (namely, they are not included in each other) clusters of sites. We denote by Γ the set of maximal clusters together with all its subclusters α, and by Φ_α the *restriction* of the Baym-Kadanoff functional to $G_\alpha(i,j)$, with $G_\alpha(i,j)=G(i,j)$ if i and j belong to α and $G_\alpha(i,j)=0$ otherwise. $\tilde{\Phi}_\alpha$ is defined recursively in terms of the Φ_α by $\Phi_\alpha=\Sigma_{\beta\subseteq\alpha}\tilde{\Phi}_\beta$ which can be inverted by the Moebius formula $\tilde{\Phi}_\alpha=\Sigma_{\beta\subseteq\alpha}(-1)^{n_\beta-n_\alpha}\Phi_\beta$ with n_α the number of sites of cluster α. An approximation scheme is uniquely fixed once a set of maximal clusters is chosen. If the chosen set is invariant under translations, e.g., the set of all plaquettes, we construct a cluster scheme which is manifestly translation invariant by truncating the full Baym-Kadanoff functional

$$\Phi\approx\sum_{\alpha\epsilon\Gamma}\tilde{\Phi}_\alpha. \tag{17}$$

Differentiation of Φ yields a translational invariant self-energy, which requires the solution of several impurity problems. The subclusters of a maximal cluster are generally related among each other by the operations of the crystal group, and fall into different equivalence classes. To compute the lattice self-energy, one needs to solve several impurity models—one for each representative of inequivalent subclusters of the maximal cluster.

When we take as a set of maximal subclusters the set of all nearest-neighbor pairs of the lattice, we obtain the pair scheme (or two-impurity scheme)[1,5] which we discuss in more detail for completeness. It is convenient to go back to a lattice notation where lattice sites are denoted by i and j and not by $R\mu$. The approximation to the Φ functional can be written in terms of Φ_1 and Φ_2 which are the Baym-Kadanoff functionals of a one- and a two-impurity problem.

$$\Phi_{\text{pair}}=(1-z)\sum_i\Phi_1[G_{ii}]+\sum_{\langle ij\rangle}\Phi_2[G_{ii},G_{jj},G_{ij}]. \tag{18}$$

Differentiating this functional gives an equation for the local self-energy and the nearest-neighbor self-energy:

$$\Sigma_{\text{loc}}=\frac{\delta\Phi}{\delta G_{ii}}=\frac{\delta\Phi_1}{\delta G_{ii}}+z\left(\frac{\delta\Phi_2}{\delta G_{ii}}-\frac{\delta\Phi_1}{\delta G_{ii}}\right), \tag{19a}$$

$$\Sigma_{nn}=\frac{\delta\Phi_2}{\delta G_{ij}}. \tag{19b}$$

The diagrammatic interpretation of the first equation is transparent: each diagram that involves a link is properly counted in the solution of a two-impurity model. The diagrams for the local self-energy at site i, which involve only the Green function at site i, can be obtained from a one-impurity model with the correct counting. The contribution of the diagrams for the local self-energy, which involve the Green functions of a pair of sites, can be obtained by subtracting the contributions from the one- and the two-impurity self-energy and multiplying by z, which results in Eq. (19a). From Σ_{loc} and Σ_{nn} we can construct the lattice self-energy.

$$\Sigma^{\text{latt}}=\Sigma_{\text{loc}}(i\omega_n)+t(k)\Sigma_{nn}(i\omega_n) \tag{20}$$

and close the equations by requiring the self-consistency condition imposed by the Dyson equation.[1]

$$G_{\text{loc}}=\sum_k\frac{1}{i\omega_n-t(k)-\Sigma_{\text{loc}}(i\omega_n)-t(k)\Sigma_{nn}(i\omega_n)}, \tag{21a}$$

$$G_{nn}=\sum_k\frac{e^{ik.\vec{\delta}}}{i\omega_n-t(k)-\Sigma_{\text{loc}}(i\omega_n)-t(k)\Sigma_{nn}(i\omega_n)}. \tag{21b}$$

This can be expressed in the matrix notation, with 2×2 matrices

$$G=\begin{pmatrix}G_{\text{loc}} & G_{nn}\\ G_{nn} & G_{\text{loc}}\end{pmatrix}$$

and K in the reduced Brillouin zone:

$$G=\sum_{K\in\text{R.B.Z.}}[i\omega_n-t(K)-\Sigma^{\text{latt}}(K)]^{-1}. \tag{22}$$

The generalization of this scheme to antiferromagnetic order is presented in Appendix D. An important feature of this scheme is that the Green function of the one-site problem coincides with the diagonal part of the Green function of the two-site problem. This is a general ''nested'' structure for these schemes, hence the name ''nested cluster schemes.'' We will see in Sec. III that this property leads to a quantitatively good classical cluster scheme.

D. Hartree-Fock terms

Another important issue is the treatment of longer-range interactions within CDMFT and PCDMFT. In this context it

is worth noticing that the Hartree-Fock contribution to the Baym-Kadanoff functional (10),

$$\Phi_{HF}[G]=\sum U_{\alpha\beta\gamma\delta}(R_1,R_2,R_3,R_4) \times[G_{\beta\alpha}(R_2R_1)G_{\delta\gamma}(R_4R_3) - G_{\delta\alpha}(R_4R_1)G_{\beta\gamma}(R_2R_3)], \quad (23)$$

induces a self-energy which is frequency independent and therefore does not cause problems with causality and can be evaluated with little computational cost. So it is convenient to separate $\Phi=\Phi_{HF}+\Phi_{\rm dyn}$, and apply the cluster DMFT truncation only to $\Phi_{\rm dyn}$, and to the self-energy it generates while treating the Hartree contributions exactly. More precisely, one can treat with Hartree-Fock terms that connect the cluster to the exterior only, to avoid a double counting problem.

This observation is particularly relevant in the treatment of broken symmetries induced by nonlocal interactions as exemplified in the study of the transition to a charge-density wave in the extended Hubbard model in one dimension which was studied in Ref. 11.

III. CLASSICAL LIMIT

In this section, in an attempt to clarify the nature of the various cluster approximations, we investigate analytically the large-U limit of the Falikov-Kimball model, which reduces to the classical Ising model in that case. The Falikov-Kimbal model is defined by the Hamiltonian

$$H=\sum_{\langle i,j\rangle} t_{ij\sigma}c^{\dagger}_{i\sigma}c_{i\sigma}+U\left(n_{i\uparrow}-\frac{1}{2}\right)\left(n_{i\downarrow}-\frac{1}{2}\right), \quad (24)$$

where $\langle i,j\rangle$ denotes nearest neighbors, $t_{ij\uparrow}=t$ and $t_{ij\downarrow}=0$. We consider the particle-hole symmetric case ($\mu=0$). This model has been studied a lot (for a review, see Ref. 20), but we will use it here as a tool to derive a classical limit for the various cluster methods. This completes the quantum Monte Carlo study of this model with CMDFT and DCA.[10] Indeed, in the limit $U\to\infty$ with $\beta\to\infty$, $\overline{\beta}=\beta t/U$ fixed, it reduces on the lattice to the Ising model at temperature $1/\overline{\beta}$:

$$H=\sum_{\langle i,j\rangle} J^{\rm Latt}_{i-j}S^z_iS^z_j, \quad (25a)$$

$$J^{\rm Latt}_{i-j}=t_{ij}/2 \quad (25b)$$

with $S^z_i\equiv(c^{\dagger}_{i\uparrow}c_{i\uparrow}-c^{\dagger}_{i\downarrow}c_{i\downarrow})$ (Ising spins). Note that a factor t/U has been absorbed in the definition of $\overline{\beta}$. The proof is analogous to the standard reduction of the Hubbard model to the Heisenberg model: since down electrons are quenched, there is no possible exchange between two spins at different sites, which implies that the interaction is Ising-like. We will now take the classical limit of the various cluster schemes, using their common expressions (2a) and (7) in order to obtain classical cluster approximations of the Ising model. For the reader not interested in the derivation, we summarize our findings in Sec. III B.

A. Derivation of the classical limit

We first present the derivation of the classical limit of CDMFT, DCA, and PCDMFT. Our results on the classical limit of the pair scheme are presented, but derived in Appendix D.

In the following, we will concentrate on square clusters on the square lattice. For clusters with an odd size it is necessary to slightly generalize the CDMFT equations to get antiferromagnetism in the usual way, distinguishing two sublattices.[1] To avoid cumbersome notations, we will discuss that point later. The key point is of course that $t_{ij\downarrow}=0$ makes the model partially solvable in the various schemes.

A priori, we have an effective action given by Eq. (3a). Since $t_{\downarrow}=0$, we can show self-consistently that $G_{0\downarrow}$ is diagonal. Indeed, if $G_{0\downarrow}$ is diagonal, because of the form of the $n_{\uparrow}n_{\downarrow}$ vertex, $G_{\downarrow}$ is diagonal (at all orders in U), and so is $\Sigma_{\downarrow}$. In all schemes, $\Sigma^{\rm latt}_{\downarrow}$ is then diagonal and independent of K. Therefore from Eq. (2a), we get for CDMFT, DCA, and PCDMFT:

$$(G_{0\downarrow})^{-1}(i\omega_n)=i\omega_n+\Sigma^{\rm C}_{\downarrow}(i\omega_n)-\Sigma^{\rm latt}_{\downarrow}(i\omega_n)=i\omega_n.$$

(For the pair scheme, see Appendix D.) Therefore we can consider $n_{\downarrow}$ as a classical variable and compute the Green function for the up electrons, solving the effective action:

$$S_{\rm eff}=-\int\int_0^{\beta}d\tau d\tau' c^{\dagger}_{\mu\uparrow}(\tau)G^{-1}_{0,\mu\nu}(\tau,\tau')c_{\nu\uparrow}(\tau') + \int_0^{\beta}d\tau c^{\dagger}_{\mu\downarrow}(\tau)\partial_{\tau}c_{\mu\downarrow}(\tau)+U\left(n_{\mu\uparrow}(\tau)-\frac{1}{2}\right) \times\left(n_{\mu\downarrow}(\tau)-\frac{1}{2}\right), \quad (26)$$

where μ,ν are intracluster indices. For fixed $n_{\downarrow}$, the action for the up electrons is Gaussian, which leads to

$$G_{\mu\nu}=\sum_{\{n_{\rho\downarrow}=0,1\}}\frac{Z(\{n_{\rho\downarrow}\})}{Z}\left[G^{-1}_{0\mu\nu}-\left(n_{\mu\downarrow}-\frac{1}{2}\right)U\delta_{\mu\nu}\right]^{-1}, \quad (27a)$$

$$Z(\{n_{\rho\downarrow}\})\equiv\exp\left\{\mathrm{Tr}\ln\left[G^{-1}_{0\mu\nu}-\left(n_{\mu\downarrow}-\frac{1}{2}\right)U\delta_{\mu\nu}\right]\right\} \times\exp\left(\beta U/2\sum_{\rho}n_{\rho\downarrow}\right), \quad (27b)$$

$$Z\equiv\sum_{\{n_{\rho\downarrow}=0,1\}}Z(\{n_{\rho\downarrow}\}). \quad (27c)$$

The computation of the large-U limit is organized in two steps. First, we find the expansion of G_0, and second we show that in this limit the effective action (27b) becomes the action for a classical Ising cluster with mean-field-like terms.

Moreover, the study of the large-U limit requires an expansion in the limit $U\to\infty$ and $\omega\to\infty$, with $x=2\omega_n/U$ fixed. Indeed there is a strong ω dependence at the scale U, as seen already in the atomic limit. We will see that the final result is *not* determined by the $x\to 0$ limit.

First, we use an ansatz for G_0, which we will prove to be consistent

$$G_0^{-1}(i\omega_n)=i\frac{U}{2}x-\Delta(x) \tag{28}$$

with Δ of the order 1 in $1/U$ (plus subdominant terms). Using the expansion

$$(\Lambda-\Delta)^{-1}=\Lambda^{-1}+\Lambda^{-1}\Delta\Lambda^{-1}+\cdots$$

with $\Lambda_{\mu\nu}=(S_\mu+ix)(U/2)\delta_{\mu\nu}$, $S_\mu\equiv 1-2n_{\mu\downarrow}$, we expand $G_\uparrow$ in Eq. (27a) and obtain from Eq. (2c) the following expansion for the cluster self-energy of the up electrons Σ^{C}:

$$\Sigma^{\mathrm{C}}_{\mu\nu}\equiv\Sigma^{\mathrm{C}\,\mathrm{diag}}_{\mu\nu}+\delta\Sigma^{\mathrm{C}}_{\mu\nu}, \tag{29a}$$

$$\Sigma^{\mathrm{C}\,\mathrm{diag}}_{\mu\nu}=-\frac{U\delta_{\mu\nu}}{2}\left(\frac{1}{\langle h_\mu\rangle}-ix\right)+O(1), \tag{29b}$$

$$\delta\Sigma^{\mathrm{C}}_{\mu\nu}\equiv(1-\delta_{\mu\nu})\Delta_{\mu\nu}\frac{\langle h_\mu h_\nu\rangle_c}{\langle h_\mu\rangle\langle h_\nu\rangle}+O\left(\frac{1}{U}\right), \tag{29c}$$

$$h_\mu\equiv\frac{1}{S_\mu+ix}, \tag{29d}$$

where $\Sigma^{\mathrm{C}\,\mathrm{diag}}$ ($\delta\Sigma^{\mathrm{C}}_{\mu\nu}$) is the diagonal (off-diagonal) part of the matrix, the brackets denote the average over $n_{\mu\downarrow}$ or S_μ with the weights defined in Eq. (27a). The averages and correlations of h_μ are computed using $S_\mu=\pm 1$ and solving for the probability of the spin to be ± 1 as a function of the correlations:

$$\langle h_\mu\rangle=\frac{\langle S_\mu\rangle-ix}{1+x^2}, \tag{30a}$$

$$\langle h_\mu h_\nu\rangle=\frac{\langle S_\mu S_\nu\rangle-ix(\langle S_\mu\rangle+\langle S_\nu\rangle)-x^2}{(1+x^2)^2}. \tag{30b}$$

For (μ,ν) nearest neighbors in an antiferromagnetic phase, as well as in the paramagnetic phase, we have $\langle S_\mu\rangle+\langle S_\nu\rangle=0$ and thus

$$\frac{\langle h_\mu h_\nu\rangle_c}{\langle h_\mu h_\nu\rangle}=\frac{\langle S_\mu S_\nu\rangle_c}{\langle S_\mu S_\nu\rangle-x^2}. \tag{31}$$

We now take the limit in the self-consistency condition (7). We keep Σ_S to derive a general formula, and we will specialize to various schemes later. We only use the fact that the diagonal part of Σ_S is independent of K and equal to the cluster self-energy: $\Sigma_{S\mu\mu}=\Sigma^{\mathrm{C}}_{\mu\mu}$. This is true for the schemes studied in this paragraph: PCDMFT, CDMFT, and DCA (for the pair scheme, see Appendix D). Therefore, the dominant part of order U in Σ_S is diagonal and we have

$$\Sigma_S(K)=\Sigma^{\mathrm{C}\,\mathrm{diag}}_{\mu\nu}+\delta\Sigma_S(K), \tag{32}$$

where $\delta\Sigma_S$ is a matrix of order $O(1)$ in the $1/U$ expansion. Denoting with a bar the normalized sum of the reduced Brillouin zone,

$$\overline{A(K)}\equiv\frac{\sum_{K\in\mathrm{R.B.Z.}}A(K)}{\sum_{K\in\mathrm{R.B.Z.}}1},$$

we obtain (R is on the superlattice)

$$\Delta_{\mu\nu}(x)=\tilde{t}_{\mu\nu}(x)+\frac{2t}{U}J^{\mu\nu}_\rho(x)\langle h_\rho\rangle+O\left(\frac{1}{U^2}\right), \tag{33a}$$

$$\tilde{t}(x)\equiv\overline{t_S}+\overline{\delta\Sigma_S}-\delta\Sigma^{\mathrm{C}}, \tag{33b}$$

$$\begin{aligned}J^{\mu\nu}_\rho(x)&\equiv\frac{1}{t}[\overline{(t_S+\delta\Sigma_S)_{\mu\rho}(t_S+\delta\Sigma_S)_{\rho\nu}}\\&\quad-\overline{(t_S+\delta\Sigma_S)}_{\mu\rho}\overline{(t_S+\delta\Sigma_S)}_{\rho\nu}]\\&=\frac{1}{t}\sum_{R\neq 0}(t_S+\delta\Sigma_S)_{\mu\rho}(R)(t_S+\delta\Sigma_S)_{\rho\nu}(-R).\end{aligned} \tag{33c}$$

Note that $\tilde{t}$ is purely off-diagonal. In the expression of J, $\delta\Sigma_S$ has to be expanded to order $O(1)$ only. Moreover, only the off-diagonal part (in site index) is important since the on-site part is restricted to $R=0$. $\delta\Sigma_S$ and Δ are determined by Eqs. (29) and (33) and the relation between Σ_S and Σ^{C}.

At this stage, it is useful to distinguish two cases depending on the validity of the cancellation

$$\overline{\Sigma_S}=\Sigma^{\mathrm{C}}. \tag{34}$$

In CDMFT and DCA, $\Sigma_S=\Sigma^{\mathrm{C}}$ is K independent, therefore Eq. (34) holds and $\delta\Sigma_S$ drops out of Eq. (33c). $\tilde{t}$ and J do not depend on x, although $\langle h_\mu\rangle$ does. In PCDMFT, however, Eq. (34) does not hold and we have to solve for $\delta\Sigma_S$ and Δ (see below) to complete the computation of G_0.

The second step of the computation is to take the large-U limit of the effective action (26) using the value of G_0 (33). In that limit, we expect that the problem becomes classical, and more precisely for $U\to\infty$:

$$\langle c^\dagger_{\sigma\mu}c_{\sigma\nu}\rangle\to 0 \quad \text{for } \mu\neq\nu, \tag{35a}$$

$$n_{\mu\uparrow}+n_{\mu\downarrow}\to 1 \quad \forall\mu. \tag{35b}$$

Indeed this can be shown explicitly using Eq. (27a) and taking the $U\to\infty$ limit in the Fermi factors, *after* doing the summation over frequencies. However, due to the frequency dependent nature of G_0 in *all* cases, we need to use the functional formalism and not the Hamiltonian formalism as in the derivation of the Ising limit on the lattice. This is presented in detail in Appendix B. In the limit $U\to\infty$ with

$\beta\to\infty$, $\overline{\beta}\equiv\beta t/U$ fixed, the effective action reduces to the classical action for the cluster *at temperature* $1/\overline{\beta}$ and we obtain a *classical cluster scheme* for the Ising model with an interaction J_{Ising} inside the cluster and an additional mean-field term J_B:

$$H_{\mathrm{eff}}=\sum_{\langle\mu,\nu\rangle}J^{\mu\nu}_{\mathrm{Ising}}S_\mu S_\nu+\sum_{(\mu,\nu)}J^{\mu\nu}_B S_\mu\langle S_\nu\rangle_{H_{\mathrm{eff}}}, \tag{36a}$$

$$J^{\mu\nu}_{\mathrm{Ising}}\equiv\int_{-\infty}^{\infty}\frac{dx}{\pi t}\frac{\tilde{t}^2_{\mu\nu}(x)}{(1+x^2)^2}, \tag{36b}$$

$$J^{\mu\nu}_B\equiv\int_{-\infty}^{\infty}\frac{dx}{\pi}\frac{J^{\mu\mu}_\nu(x)}{(1+x^2)^2}, \tag{36c}$$

where (μ,ν) and $\langle\mu,\nu\rangle$ correspond to a general and a nearest-neighbor couple of sites, respectively. One has to solve a classical Ising cluster, with self-consistent ''boundary'' condition represented by J_B, which generalizes the usual Weiss field. Of course, if $\tilde{t}$ does not depend on x, we find the same result as in the lattice $J^{\mu\nu}_{\mathrm{Ising}}=J^{\mathrm{Latt}}_{\mu-\nu}$ for nearest neighbors.

Let us now specialize our computations to the three schemes presented in Sec. II and compute the value of J_{Ising} and J_B for CDMFT, DCA, and PCDMFT for square clusters of linear size L on a two-dimensional square lattice and for a general hopping t_δ where δ is a lattice vector.

CDMFT. In this case, $\Sigma_S(K)=\Sigma^{\mathrm{C}}$ is K independent and $t_S=t$, which leads to $\tilde{t}(x)=t$ and

$$J^{\mu\nu}_{\mathrm{Ising}}=J^{\mathrm{Latt}}_{\mu-\nu}, \tag{37a}$$

$$J^{\mu\nu}_B=(-1)^L\sum_{R\neq 0}J^{\mathrm{Latt}}_{\mu-\nu+R}. \tag{37b}$$

The interaction inside the cluster is the same as in the lattice problem and the J_B term is of order $O(1)$ and is confined to the boundary of the cluster. The boundary term couples a spin to the average value of its ''ghost'' neighbor in the neighboring cells, this average value being computed in the cluster itself using the translation invariance on the superlattice. We added a ''$-$'' sign for odd cluster size, since in this case the CDMFT has to be generalized like DMFT with two sublattices in order to capture antiferromagnetism: this is equivalent to reversing the sign of the ghost neighbor. In the large cluster limit $L\to\infty$, the boundary terms play no role and we therefore recover the lattice Ising problem. Notice, however, that the one-dimensional case is pathological since the two boundary terms communicate with each other, resulting in a finite T_c in the limit of infinite size. This pathology disappears in higher dimensions and explains the results of Ref. 10.

DCA. In $d=2$, we use a square cluster of linear size $L=2L_c$, corresponding to L_cK_c points (cf. Appendix A). With the definition $\mathrm{sin}_c(\vec{x})\equiv\Pi_{i=1}^d\sin(x_i)/x_i$:

$$J^{\mu\nu}_{\mathrm{Ising}}=\frac{t}{2}\left[\sum_{\delta=\mu-\nu[2L_c]}\frac{t_\delta}{t}\mathrm{sin}_c\left(\frac{\pi\delta}{2L_c}\right)\right]^2, \tag{38a}$$

$$J^{\mu\nu}_B=\frac{t}{2}\sum_{\substack{\delta,\delta'\\ \delta=\mu-\nu[2L_c]\\ \delta'=\mu-\nu[2L_c]}}\frac{t_\delta t_{-\delta'}}{t^2}\mathrm{sin}_c\left(\frac{\pi(\delta-\delta')}{2L_c}\right)-J^{\mu\nu}_{\mathrm{Ising}}. \tag{38b}$$

J_B is the same for all links as required by translation invariance in the cluster. For the first-neighbor hopping, denoting by J^{Latt} the value of J^{Latt}_{i-j} for i,j nearest neighbors, the formula reduces to

$$J^{\mu\nu}_{\mathrm{Ising}}=\frac{16}{\pi^2}J^{\mathrm{Latt}},\quad J^{\mu\nu}_B=\left(2-\frac{16}{\pi^2}\right)J^{\mathrm{Latt}}\quad\text{for } L_c=1, \tag{39a}$$

$$J^{\mu\nu}_{\mathrm{Ising}}=\left(\mathrm{sin}_c\frac{\pi}{2L_c}\right)^2J^{\mathrm{Latt}},$$

$$J^{\mu\nu}_B=\left[1-\left(\mathrm{sin}_c\frac{\pi}{2L_c}\right)^2\right]J^{\mathrm{Latt}}\quad\text{for } L_c>1. \tag{39b}$$

Note that in the 2×2 cluster, the hopping is doubled since electrons can hop from one site to the neighboring one, either directly or using the cyclicity condition. In the large cluster limit $L_c\to\infty$, we recover the lattice problem: $J^{\mu\nu}_{\mathrm{Ising}}\to J^{\mathrm{Latt}}_{\mu-\nu}$ and $J_B=O(1/L_c^2)$.[10]

PCDMFT. This case is more complicated since $\Sigma_S=\Sigma^{\mathrm{latt}}$ is now K dependent, hence $\overline{\Sigma_S}\neq\Sigma^{\mathrm{C}}$, except for diagonal elements. Therefore t and J now depend on x. In order to determine them, we have to solve Eqs. (9), (29), and (33). This is done in Appendix C and we obtain

$$\tilde{t}_{\mu\nu}(x)=t_{\mu\nu}\frac{\langle h_\mu\rangle\langle h_\nu\rangle}{A(x)\langle h_\mu h_\nu\rangle}, \tag{40a}$$

$$J^{\mu\mu}_\nu(x)=(-1)^LA^{-2}(x)\sum_{R\neq 0}\frac{t^2_{\mu-\nu+R}}{t}, \tag{40b}$$

$$A(x)\equiv 1-\frac{1}{S_c}\sum_{\substack{\rho\in\mathcal{C}\\ \rho+\delta\in\mathcal{C}}}\frac{\langle h_\rho h_{\rho+\delta}\rangle_c}{\langle h_\rho h_{\rho+\delta}\rangle}, \tag{40c}$$

where δ is one of the basis vectors of the square lattice.

In $d=1$ for first-neighbor hopping, the last term reduces to

$$A(x)=1-\frac{1}{L}\sum_{i=1}^{L-1}\frac{\langle h_ih_{i-1}\rangle_c}{\langle h_ih_{i-1}\rangle}.$$

The boundary terms are located as in CDMFT. In the large cluster limit $L\to\infty$, in Eq. (40) the boundary terms are subdominant in the denominator and the terms involving the averages of S cancel, restoring the correct J_{Ising} on the lattice. The J_B term cancels since it is restricted to the boundary.

Pair scheme. The computation of the classical limit of the pair scheme is a little more involved but similar. We show in Appendix D that if a magnetic solution exists, it satisfies the equation of the classical variation method. Let us take two cluster problems, the first one with one site [denoted with an index (1)] in a field $-zh$, the second one with two sites [denoted with an index (2)], interacting antiferromagnetically with J^{Latt} and in a field $-(z-1)h$, where $z=4$ is the connectivity:

$$H^{(1)}=zhS^{(1)}, \tag{41a}$$

$$H^{(2)}=(z-1)h(S_1^{(2)}-S_2^{(2)})+J^{\mathrm{Latt}}S_1^{(2)}S_2^{(2)}, \tag{41b}$$

where the field h is determined by the ''nested consistency condition''

$$\langle S^{(1)}\rangle=\langle S_1^{(2)}\rangle=-\langle S_2^{(2)}\rangle. \tag{42}$$

Solving the classical equations, the critical temperature is given by

$$(z-1)\tanh(\overline{\beta}J^{\mathrm{Latt}})=1, \tag{43}$$

which gives $\overline{T_c}/J^{\mathrm{Latt}}\approx 2.88$.

B. Discussion

Let us recapitulate our results. We applied the cluster dynamical mean-field theories to the Falikov-Kimball model taking $U\to\infty$ with $\beta\to\infty$, $\overline{\beta}=\beta t/U$ fixed. In this case the quantum model reduces to the Ising model and the cluster dynamical mean-field approximation to classical cluster methods. CDMFT corresponds to a simple mean-field theory generalized to clusters: each spin on the boundary is subjected to a mean field representing the interaction with the neighboring spins that do not belong to the cluster. The form of the mean field is the standard one: the antiferromagnetic coupling times the magnetization of the spins. Note that, in principle, the antiferromagnetic coupling is generated via quantum fluctuations and its value is approximation dependent. In the case of CDMFT one gets the same coupling as the one obtained for the lattice.

The classical limit of DCA is different mainly for two reasons:

(i) The mean field is not just on the boundary but it acts on all sites and is equal on sites belonging to the same sublattice. This is natural in DCA because it is an approximation that preserves the translation invariance (or the reduced translation invariance for the AF phase), in the propagator and in the Weiss field;

(ii) The form of the mean field is the standard one but the values of the antiferromagnetic coupling in the mean field and for spins inside the cluster are different from the lattice one (and between themselves). Of course, in the limit of infinite cluster they reduce to the lattice value.

PCDMFT is similar to CDMFT to the extent that the mean field acts only on the boundary. However, as for DCA, the value of the antiferromagnetic coupling in the mean field and for spins inside the cluster are different from the lattice one (and between themselves). Finally, the pair scheme reduces to the classical cluster variation method for two sites.

The self-consistent equations corresponding to these classical cluster schemes can be solved analytically for small clusters and using a classical Monte Carlo method to solve the impurity problem for larger size. With the exception of the cluster variational method, the classical limits of these extensions of DMFT do not result in drastic improvements in the estimation of T_c for small cluster sizes. The value of T_c predicted by DMFT is the standard mean-field one: $4J$ (the connectivity of the lattice is four), which is far from the exact value of $2.27J$. The value obtained using the NCS scheme with two sites, i.e., the pair scheme, leads to a good improvement: $T_c=2.88J$. Instead the results for DCA and CDMFT even for larger sizes (4×4, 6×6, and 8×8 clusters) do not improve the estimate of T_c very much. In fact, within error bars of 0.1 we get $T_c^{(4\times 4)}=3.2J$, $T_c^{(6\times 6)}=3.J$, and $T_c^{(8\times 8)}=2.85J$ (within the error bars the estimates for T_c are the same for the two schemes). Note that the value obtained with a cluster of 16 sites with DCA and CDMFT reaches the estimate obtained with a cluster of two sites using NCS! The results of PCDMFT are clearly worse than the ones of the two previous methods for the numerical value of T_c, which is quite larger than what is obtained by CDMFT and DCA. This can be traced to the lack of cancellation of off-diagonal elements in Eq. (34) which implies that the cavity field $\Delta(i\omega_n)$ in PCDMFT is not proportional to the square of the hopping matrix element which is an undesirable feature.

IV. CAUSALITY

In this section, we present a general method to prove the causality of cluster approximations and apply it to various schemes, including PCDMFT. As mentioned in Sec. II, there are two equivalent presentations for the equations of DMFT and its extensions: a first one using the Weiss function G_0, and another one using the Luttinger-Ward functional Φ. Let us examine the causality question in both.

In the formulation with G_0, one has to prove that (i) if G_0 is causal, G_c and Σ are causal (this is automatic as long as one uses a causal impurity solver), (ii) if Σ is causal, G_0 computed from the self-consistency condition is causal. This is the difficult part. It was carried out explicitly for CDMFT in Ref. 9 and for DCA in Ref. 7.

In the formulation with Φ, one has to prove that (i) given a causal G, $\Sigma_{\mathrm{skel}}(G)=\delta\Phi/\delta G$ is causal; (ii) given a causal Σ, the self-consistency condition produces a causal G. Here (ii) is obvious, because of the simple form of the bare propagator. (i) is the difficult part and this section is devoted to a general method to prove it.

To show that the self-energy is causal we have to prove that the retarded self-energy has a negative imaginary part for all ω, i.e., $\mathrm{Im}\,\Sigma_R(x,x',\omega)\equiv[\Sigma_R(x,x',\omega)-\Sigma_R^*(x',x,\omega)]/2i$ is negative. We use the Cutkovsky-t'Hooft-Veltman equation (also known in the literature as ''cutting equations'') which is extremely useful to discuss causality properties in terms of a diagrammatic expansion. It relates the imaginary part of the self-energy to a sum of cut diagrams. A standard derivation can be found in Ref. 21 and

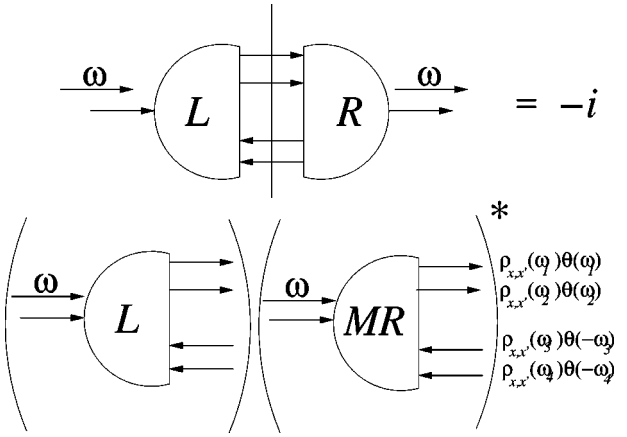

FIG. 1. Definition of cut diagrams.

it is proposed by t'Hooft and Veltman. However, we present in Appendix E a simpler and self-contained derivation, based on the Keldysh method. Contrary to the previous derivation, it does not assume translation invariance, which is important to discuss cluster schemes that break translation invariance. Note, however, that this method is limited to zero-temperature formalism.

This section is organized as follows. In Sec. IV A, we present the Cutkovsky-t'Hooft-Veltman equation and show how it can used to prove causality. In Sec. IV B, we apply it to various cluster schemes.

A. The Cutkovsky-t'Hooft-Veltman equation

The Cutkovsky-t'Hooft-Veltman equation gives the imaginary part of the retarded self-energy as a sum of cut diagrams. Let us consider the set of all perturbative connected diagrams $\{D\}$ for the self-energy at zero temperature (for a given approximation) and all possible cuts of these diagrams into two connected parts L and R containing, respectively, the left and the right external points (if they are the same, we drop the diagram). There are n cut propagators going from left to right and $n-1$ from right to left, at frequency ω_i and indices x_i. We denote by MR the mirror of R defined as the left diagram obtained from R by reversing all arrows (cf. Fig. 1 for an illustration). To each left diagram, we associate the value d_L of corresponding $T=0$ diagram, using the $T=0$ Feynman propagator (G^{++} in Keldysh notation: See Appendix E). Note that for each given half left diagram, one has to put in d_L all the half left diagrams obtained by permuting the cut lines in all the possible ways and then multiply by an appropriate symmetry factor discussed in Appendix E. We then write $D_L(x,\omega,\{x_i\},\{\omega_i\}) \equiv d_L\theta(\omega) + d_L^*\theta(-\omega)$, where θ is the Heaviside function. We denote all cut propagators with an index i. To each we associate $\rho(x_i,x_i',\omega_i)\theta(\epsilon_i\omega_i)$ with $\epsilon_i=\operatorname{sgn}\omega$ for a propagator going to the right and $-\operatorname{sgn}\omega$ for a propagator going to the left. The summation over diagrams can be expressed as a summation over n and a sum over diagrams $D_n=(L_n,R_n)$ with a given number of cut propagators going to the right. The Cutkovsky-t'Hooft-Veltman equation is then

$$\begin{aligned}\operatorname{Im}\Sigma_R(x,x',\omega) &= -\sum_{n\geqslant 2}\frac{1}{2n!}\sum_{D_n=(L_n,R_n)}\sum_{\substack{\{x_i\}\\ \{x_i'\}}}\int d\omega_i D_{L_n}(x,\omega,\{x_i\},\{\omega_i\})\\ &\times[D_{MR_n}(x',\omega,\{x_i'\},\{\omega_i\})]^*\\ &\times\prod_{i=1}^{n_L+n_R}\rho(x_i,x_i',\omega_i)\theta(\epsilon_i\omega_i). \end{aligned} \tag{44}$$

Remark. If the system is translation invariant then we can Fourier transform also with respect to space and get

$$\begin{aligned}\operatorname{Im}\Sigma_R(k,\omega) &= -\sum_{n\geqslant 2}\frac{1}{2n!}\sum_{D_n=(L_n,R_n)}\sum_{\substack{\{x_i\}\\ \{x_i'\}}}\int d\omega_i\\ &\times D_{L_n}(k,\omega,\{k_i\},\{\omega_i\})\\ &\times[D_{MR_n}(k,\omega,\{k_i\},\{\omega_i\})]^*\\ &\times\prod_{i=1}^{n_L+n_R}\rho(k_i,\omega_i)\theta(\epsilon_i\omega_i). \end{aligned} \tag{45}$$

Note that there are no terms with $n\leqslant 2$, otherwise the original closed diagram would not be two-particle irreducible (2PI).

Let us now see how to use Eq. (44) to prove causality of the self-energy. We want to show that

$$\mathcal{A}=\frac{1}{2i}\sum_{x,x'} w_x[\Sigma_R(x,x',\omega)-\Sigma_R^*(x',x,\omega)]w_{x'}^*\leqslant 0 \quad \forall\{w_x\} \tag{46}$$

for all complex vectors w_x. Using Eq. (44) we find that we can write the previous quantity as a sum over cut diagrams:

$$\begin{aligned}\mathcal{A} &= -\sum_{\substack{n_L\geqslant 0\\ n_R\geqslant 0}}\frac{1}{2n!}\sum_{D_n=(L_n,R_n)}\sum_{\substack{\{x_i\}\\ \{x_i'\}}}\int d\omega_i\\ &\times\left(\sum_x w_x D_{L_n}(x,\omega,\{x_i\},\{\omega_i\})\right)\\ &\times\left(\sum_{x'} w_{x'}^* D_{MR_n}^*(x',\omega,\{x_i'\},\{\omega_i\})\right)\\ &\times\prod_{i=1}^{n_L+n_R}\rho(x_i,x_i',\omega_i)\theta(\epsilon_i\omega_i). \end{aligned} \tag{47}$$

At this stage, we can use the causality of G, i.e., the positivity of $\rho(x,x')$. It implies the positivity of the tensor product $\Pi_{i=1}^{n_L+n_R}\rho(x_i,x_i',\omega_i)$ considered as a matrix of indices $(x_1,\ldots,x_{n_L+n_R})$. Hence, positivity of $-\operatorname{Im}\Sigma$ would result if the summation over diagrams could be recast as a square. More precisely, a simple property that implies causality is that for any n

$$\{(L_n,R_n)\}=\{L_n\}\times\{R_n\}. \tag{48}$$

$\{L_n\}$ ($\{R_n\}$) is the set of left (right) parts of diagrams with fixed n. Equation (48) says that all diagrams can be obtained once and only once using a left part and a right part, which is equivalent to two properties:

Closure property. With any left part and any right part (which have the same n), gluing them constructs a diagram present in the expansion.

Exact counting property. All diagrams are obtained that way (by definition of left/right parts) but only once: there is no overcounting problem.

If the property (49) holds, then using the notation

$$y_n(\{x_i\};\{\omega_i\},\omega)\equiv\sum_{x,L_n} w_x D_{L_n}(x,\omega,\{x_i\},\{\omega_i\}),$$

we have

$$\mathcal{A}=-\int d\omega_i \sum_{n\geqslant 2}\sum_{\{x_i\},\{x_i'\}} y_n(\{x_i\};\{\omega_i\},\omega)y_n^*(\{x_i'\};\{\omega_i\},\omega) \times\prod_{i=1}^{n_L+n_R}\rho(x_i,x_i',\omega_i)\theta(\epsilon_i\omega_i). \tag{49}$$

Note that the sum over $\{x_i\},\{x_i'\}$ inside the integral can be interpreted as the product of the two vectors y and y^* with a positive definite matrix. Thus the positivity of ρ implies the negativity of $\mathrm{Im}\,\Sigma$.

The efficiency of this method is that one can prove causality, just by examining the combinatoric structure of the diagrams present in the approximation, with no further computation. A few remarks are important at this stage.

(i) This method can prove the causality of a scheme, but it cannot prove that a scheme will violate causality. In particular, it proves the positivity of $-\mathrm{Im}\,\Sigma$ for all causal propagators G. In the following, we will refer to this as the strong causality property. It is a logical possibility that this property does not hold, while the actual solution of the scheme G is indeed causal for all parameters. However, we know no example of this, and the strong property is interesting since we use an iterative algorithm to solve the self-consistent impurity problem.

(ii) Equation (48) is sufficient but not necessary: one could also have form squares in a more complicated manner.

(iii) As a remark, we see that the full perturbation theory on the lattice satisfies the property (48): the full diagrammatic expansion obviously leads to a causal self-energy.

B. Applications

1. CDMFT and DCA

CDMFT can be obtained from the Baym-Kadanoff functional taking $\Phi=\Sigma_{\mathbf{R}}\Phi(G_{\alpha,\beta;\mathbf{R},\mathbf{R}})$, where R is the cluster index and α is the internal cluster index. As a consequence, $\Sigma_{\alpha,\beta;\mathbf{R},\mathbf{R}}=\Sigma_{\alpha,\beta}=\delta\Phi/\delta G_{\alpha,\beta}$. Since $\Phi(G_{\alpha,\beta})$ is the sum of all the 2PI diagrams of a L^d lattice, CDMFT does satisfy Eq. (48) and therefore is a causal scheme.

In DCA, one writes the self-energy in terms of the complete series of diagrams and the δ functions at the vertices are replaced by a coarse-grained function. As discussed previously, DCA is equivalent to replacing the Kronecker delta $\delta_{k_1+k_2,k_3+k_4}$ with a Kronecker delta $\delta_{k_1^c+k_2^c,k_3^c+k_4^c}$ where k_i^c is the cluster momentum related to the hypercube containing k_i. Formally $k_i^c=k_i \bmod(\pi/L,\ldots,\pi/L)$. Hence, DCA satisfies Eq. (48): the proof is the same that for the complete series of diagrams for the self-energy. The fact that the k structure of the vertices is different does not change anything. Hence, we see that DCA is automatically causal.

2. PCDMFT

The causality of PCDMFT is easily established using its real-space formulation (9). The causality for CDMFT implies the causality of Σ^{C}. We just have to show that Σ^{latt} is causal. For any complex vector $x_{\sigma\mu}$, we have from Eq. (9),

$$\sum_{\sigma\sigma'\mu\nu} x_{\sigma\mu}^* x_{\sigma'\nu}\Sigma^{\mathrm{latt}}_{\sigma,\mu;\sigma',\nu}(K) = \frac{1}{S_c}\sum_{\delta\in\{0,\ldots,L-1\}^d}\sum_{\sigma\sigma'\overline{\mu\nu}} z^*_{\sigma;\overline{\mu}}(\delta) \times z_{\sigma';\overline{\nu}}(\delta)\Sigma^{\mathrm{C}\alpha(\delta)}_{\sigma,\overline{\mu};\sigma'\overline{\nu}} \tag{50a}$$

$$z_{\sigma;\overline{\mu+\delta}}(\delta)\equiv x_{\sigma\mu}e^{iK[(\mu+\delta)/L]L}. \tag{50b}$$

The negativity of Σ^{C} implies that we have a sum of negative terms. This shows that causality of PCMDFT is guaranteed term by term in the δ sum.

Note that another way to reach the same conclusion is based on the fact that PCDMFT can be interpreted as the solution of a real lattice system replacing the real $U(k_1,k_2,k_3,k_4)$ with its PCDMFT counterpart. Thus, the statement of causality of PCDMFT is a particular case of the causality of the original problem with a general U.

3. Noncausality of the pair scheme

The pair scheme, described in Sec. II C, has been originally introduced in Refs. 1 and 5. It seems a very natural way to introduce systematically a k dependence for the self-energy. Unfortunately, as we will show in the following, this scheme is not causal for two reasons that we shall discuss in detail.

First, let us apply the Cutkovsky rule. We see that the pair scheme does not satisfy the property (48) or more precisely the closure property. Indeed, when cutting a diagram for Σ, we only have two site indices i and j. Let us consider a cut diagram $(L1,R1)$ where we have i along the cut, and the similar diagram $(L2,R2)$ where j is replaced by $k\neq i,j$. *A priori*, we could glue the parts into $(L1,R2)$, but that diagram would involve i, j, and k, and thus is not present in the diagrammatic expansion generated by the pair scheme. This is the first reason for lack of causality. We stress that this is not a proof, but a quick and strong indication that the scheme is not strongly causal. It is interesting to point out that this problem was already encountered in the case of disordered electron systems when people tried to generalize CPA to clusters. In that case Mills and collaborators[15] noticed that a generalization of CPA similar to the pair scheme has this

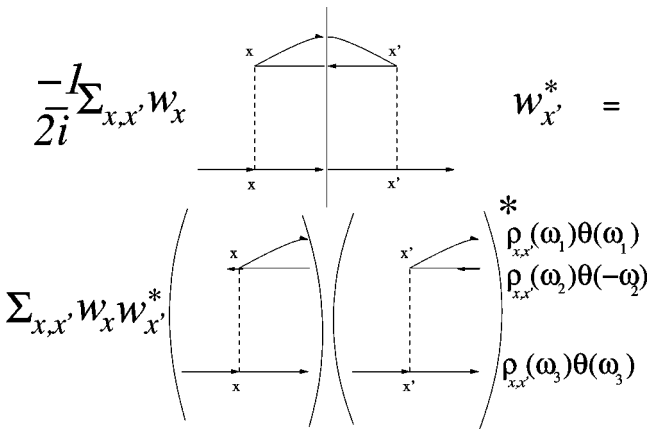

FIG. 2. Example of a cut diagram. MR means mirror image of *R*.

type of nonclosure problem. For this reason they introduced the traveling cluster method which is fully causal. We will comment afterward on the possibility to do the same for strongly correlated electrons.

Let us now really show that the pair scheme is not causal. In fact, the violation of the closure property is just a hint that there could be some problem with causality but it does not preclude the possibility that eventually the scheme is causal. In the following we will consider the solution of the pair scheme when $U\rightarrow 0$ for an arbitrary bare spectral density or hopping on the original lattice. We will show that a particular choice of the bare spectral density gives rise to a noncausal self-energy, thus proving in an explicit example the noncausality of the scheme.

To study the sign of the imaginary part of the self-energy in the limit $U\rightarrow 0$ one can focus just on the second-order term because the first order gives no contribution. Moreover, one can replace in the diagram the full propagator with the bare or lattice one $[G_{\text{bare}}=(i\omega_n - t-\mu)^{-1}]$, the error leading to a term of an order larger than $O(U^2)$. If one applies the Cutkovsky equations to obtain the imaginary part of the self-energy for the second-order diagrams of the pair scheme then one has to restrict the sum in the first line of Fig. 2 to single sites (x,x) and links $\langle x,x'\rangle$. The sum over the single sites (x,x) is just the same that one obtains for usual DMFT and is clearly positive. The link term $\langle x,x'\rangle$ with x,x' nearest neighbors equals [ω is the (positive) self-energy frequency]

$$U^2\int_0^{+\infty} d\omega_1 \int_{-\infty}^{0} d\omega_2 \sum_{\langle x,x'\rangle} [w_x w_{x'}^* \rho(x,x',\omega_1) \times \rho(x,x',\omega_2)\rho(x,x',\omega-\omega_2-\omega_3) + w_{x'} w_x^* \times \rho(x',x,\omega_1)\rho(x',x,\omega_2)\rho(x',x,\omega-\omega_2-\omega_3)]. \tag{51}$$

The spectral density in the previous equations is just the bare spectral density obtained by t_{ij}. For the pair scheme, one can find a spectral density matrix that, injected into the previous equations, does not lead to a causal self-energy. The causality of the spectral density matrix is equivalent to the positivity of each Fourier element $\rho_k(\omega)\geqslant 0$. However, even if $\rho_k(\omega)\geqslant 0$, $\rho_{x,x'}(\omega)$ with x,x' nearest neighbors can be negative and as close as possible (in absolute value) to $\rho_{x,x}(\omega)$ for any ω. Consider, for example, the example in which $\rho_k(\omega)$ is strongly peaked and has an important weight only near the points $\pm\pi,\ldots,\pm\pi$. In this case $\rho_{x,x}(\omega) > 0$, $\rho_{x,x'}(\omega)$ with x,x' nearest neighbors is negative and

$$\rho_{x,x'}(\omega) = \int_{BZ} \frac{dk}{(2\pi)^d} \rho_k(\omega) \exp[-ik(x-x')]$$

$$\simeq -\int_{BZ} \frac{dk}{(2\pi)^d} \rho_k(\omega) = -\rho_{x,x}(\omega).$$

In this case the contribution of Eq. (51), for example, for $w_x=1$, is negative and approximatively two times larger in absolute value than the contribution from the x,x term. Since for each x,x term there are z (z is the connectivity) terms like Eq. (51), the global sum is negative for $z>2$, i.e., in any dimension large than 1 (if one takes a square or cubic or hypercubic lattice). Thus in this case, the self-energy is not causal. So we have found a second reason for noncausality: even if the closure property is verified and in the cutting-folding procedure no new diagrams are created (which is the case for the pair scheme at second order in U) this does not guarantee that there is a way to write all the cut diagrams as a sum of squares. One can have an overcounting problem as we have just shown for the pair scheme.

Let us now comment on the possibility to cure the pair scheme as Mills and collaborators did in the case of disordered electrons defining the traveling cluster scheme. What they did is to solve the violation of the closure property allowing an arbitrary self-energy diagram to have only single-site and nearest-neighbor propagators. So in this case a self-energy diagram can connect two arbitrary points but just through a sequence of nearest-neighbor propagators (that is why the scheme is called ''traveling''). This clearly solves the first problem—the nonclosure—but, in principle, it does not guarantee that the second one is also solved. And indeed it is not for strongly correlated electrons. A simple way to see it is that even with a generalization of this type in the limit $U\rightarrow 0$, the causality counterexample exhibited for the pair scheme is still valid. Instead, the case of disordered electrons has a simpler diagrammatics (there are no loops in the self-energy diagrams due to the use of the replica method) and one can explicitly rewrite everything as a sum of squares. In particular, the diagram discussed before is simply not there.

A way to circumvent these two difficulties is to write the self-energy as the sum of all diagrams and then replace the original propagator with a simplified restricted version that is guaranteed to be causal. For example, in order to have a causal generalization of the pair scheme, close in spirit to the traveling cluster, one can write

$$\Sigma = \left.\frac{\delta\Phi}{\delta G}\right|_{G=\tilde{G}}, \quad \tilde{G}(k,\omega) = G_0(\omega) + G_1(\omega)\sum_{i=1}^{d} [2\cos(k_i)],$$

where G_0, G_1 are fixed imposing the conditions $\tilde{G}(0,\ldots,0,\omega)=G(0,\ldots,0,\omega)$ and $\tilde{G}(\pi,\ldots,\pi,\omega)=G(\pi,\ldots,\pi,\omega)$, and $G=(G_0^{-1}-\Sigma)^{-1}$. This guarantees that $\tilde{G}$ is a causal propagator as long as G is causal. So when $\tilde{G}$ is inserted in the complete series, it will give rise to a causal self-energy. The problems with this scheme are the following

(1) It seems that it is not Φ derivable. The reason is that in all the diagrams there are only nearest-neighbor propagators. However, since the diagrams connect, in general, two sites that are not nearest neighbors, it is difficult to think how one can obtain it using a restricted set of diagrams for Φ. Note, however, that this is also the case of the traveling cluster scheme for disordered electrons.

(2) It is not clear what type of impurity solver, if any, can be used to sum the series of diagrams.

In the case of the traveling cluster many simplifications arise that allow one to solve (2) but not (1). Let us finally remark that the two mechanisms behind the noncausality of the pair scheme apply also to the general NCS schemes, even though we expect smaller violations of causality for larger clusters.

V. CONCLUSION

Cluster schemes are a promising method for studying strongly correlated electrons. Compared to the study of small finite-size systems, they offer the advantage that the thermodynamical limit is taken from the outset, and hence one can hope for smaller finite-size effects. As a prime example, we now know that even a one-site cluster captures many nontrivial features of the Mott transition.

On the other hand, there is no unique generalization of the single-site dynamical mean-field approximation. Some generalizations view the DMFT and its resulting impurity (or multiple impurity models in the case of the NCS) as a trick for summming selected classes of diagrams. An alternative view is provided by the cavity construction and by functional methods, where an effective action is constructed to compute the correlation functions of selected coarse grained or cluster degrees of freedom. Finally, one can view DMFT as a choice of boundary condition for finite-size studies of a small set of degrees of freedom, where the boundary condition recognizes that those degrees of freedom are periodically repeated in a medium. While all those points of view lead to the same set of DMFT equations in the single site case, they lead to different constructions for cluster extensions, and the strengths and limitations of these extensions need to be explored. This paper contributed in this direction by clarifying two important aspects of these extensions, namely, the conditions on the cluster scheme needed for the scheme to satisfy causality, and the reduction of the cluster schemes to spin cluster methods in the classical limit.

First, we introduced PCDMFT which is a causal generalization of the scheme proposed by Lichtenstein and Katsnelson.[13] Second, we provided a general way to prove causality of cluster scheme and showed that the pair scheme, which is the most natural extension in the sense that it is defined by a translational invariant restriction of the Baym-Kadanoff functional, is not causal: the diagrammatic reason for the failure of this method was clarified. Third, we also showed formally, in the context of the Falikov-Kimball model, how the semiclassical limit of the different cluster methods reduces to classical spin cluster methods. Both DCA and CDMFT give comparable answers, even though their Weiss fields have a very different form (in DCA the Weiss field is uniformly distributed inside the cluster while in CDMFT it is focused on the boundary). On the other hand, PCDMFT has an unphysical feature in the classical limit which results from a Weiss field which does not vanish as the square of the hopping matrix elements. The nested cluster schemes are clearly superior and provide a quantum generalization of the cluster variation method which gives critical temperatures that converge rapidly with cluster size. We showed that the nested cluster schemes violate causality. Our proof suggests that this violation is going to be more severe when a substantial part of the lattice self-energy has a range that exceeds the size of the maximal cluster used in the NCS. On the contrary, when the range of the self-energy is contained in the maximal cluster, the diagrams generated by the Cutkovsky procedure which are not contained in the NCS are small, which is consistent with the early numerical studies which indicated no violation of causality in the pair scheme at high temperature. This observation is in the same spirit as a recent study of a new (non-nested) scheme, the ''fictive impurity model method,'' which connected violation of causality with peaks in momentum space in the lattice self-energy.[22]

An important lesson that can be learned from our results is that the choice of an optimal cluster scheme may depend of the property studied and the physical system at hand. Indeed, our semiclassical analysis revealed that PCDMFT is not accurate in insulating regimes, at least in the one that we focused on doing the semiclassical limit. Instead, CDMFT performs rather well. We conjecture that CDMFT is accurate in insulating cases and PCDMFT in metallic cases, as suggested by a recent study in one dimension.[23]

Another important result concerns the remarkable accuracy of the NCS scheme compared to the other ones. Even if its performance in a case with stronger quantum fluctuations remains an open question, we think that it would be particulary interesting to try to cure the causality problem keeping the nesting idea inherent to the NCS scheme. Another route to follow is to try to incorporate the cellular dynamical mean-field ideas of defining impurity models in adaptive basis sets into a NCS scheme. In this way one could try to adapt the basis to the problem so that the resulting self-energy is short range and the causality problem, even if not avoided, is sensibly reduced.

Finally, while the paper focused on a few schemes, the techniques developed here are quite general and may play an important role in selecting and optimizing cluster methods for specific applications.

ACKNOWLEDGMENTS

We thank A. Lichtenstein, A. Georges, S. Florens, and S. Biermann for useful discussions, and M. Jarrell for pointing

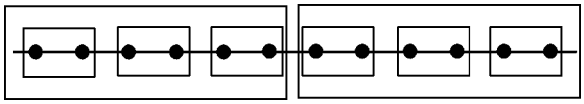

FIG. 3. Definitions of big and small clusters in $d=1$. $L=2$, $L_c=3$.

to us Ref. 16. This work was supported by NSF Grant No. DMR-0096462. We acknowledge the warm hospitality of the KITP program on Realistic Studies of Correlated Electrons, at UCSB (NSF Grant No. PHY 99-07949), where part of this work was carried out, and thank the participants of this workshop for discussions. G.B. and O.P. were supported by an ''ACI'' grant of the French Minister of Research.

APPENDIX A: REAL-SPACE FORMULATION OF DCA

In this appendix, we present a real-space formulation of DCA,[8] which is useful for orders that break translation invariance. Let us consider first the translation invariant case. The hopping of the full lattice can be written using the reciprocal superlattice and the cluster indices (in real space):

$$t_{\mu\nu}(K)=\frac{1}{L^d}\sum_{K_c} e^{i(K+K_c)(\mu-\nu)}t(K+K_c), \tag{A1}$$

where $t(k)$ is the Fourier transform of the hopping on the original lattice and μ,ν as in Sec. II. Here (in $d=1$), $-\pi/L\leqslant K\leqslant \pi/L$, $K_c=2\pi n/L$, $n=0,\ldots,L-1$ is on the reciprocal lattice of the (finite) cluster. Using $t_S=t$ in Eq. (7), we get CDMFT. Using $t_S=t^{\mathrm{cyc}}$ with

$$t^{\mathrm{cyc}}_{\mu\nu}(K)\equiv\frac{1}{L^d}\sum_{K_c} e^{iK_c(\mu-\nu)}t(K+K_c) \tag{A2a}$$

$$=e^{-iK\mu}t_{\mu\nu}(K)e^{iK\nu} \tag{A2b}$$

we get DCA. Indeed, t^{cyc} is cyclic in the cluster indices (by definition of K_c), and provided that we obtain a translation invariant (cyclic) solution we can diagonalize all matrices in the cluster to get Eq. (5).

Let us now consider the case where the solution of the real-space formulation of DCA breaks the translation invariance in the cluster into a smaller invariance: the (big) cluster is divided into L_c^d small clusters of linear size L, and we have translation invariance in the big cluster when the small clusters are thought as collapsed into one point. For example, for AF order in $d=1$, $L=2$ (see Fig. 3). We will then denote by α,β the positions in the small cluster, by A,B the positions of the small clusters in the big clusters, and by $\overline{A},\overline{B}$ the positions of the big clusters on the full lattice *expressed in units of the original lattice*. Any point on the big cluster can be described with a couple (α,A) and any point on the lattice by a triplet $(\alpha,A,\overline{A})$ (α, A, $\overline{A}$ designate both the position of the points, i.e., vectors, and a label for those points). Similarly, we denote by $-\pi\leqslant k\leqslant\pi$ an element of the original lattice's Brillouin zone, by $-\pi/L\leqslant K\leqslant\pi/L$ an element of the Brillouin zone of the superlattice of the small clusters, and by $-\pi/(LL_c)\leqslant\overline{K}\leqslant\pi/(LL_c)$ an element of the Brillouin Zone of the superlattice of the big clusters. Finally, the reciprocal lattice of the small cluster is $K_c=2\pi n/L, n=0,\ldots,L-1$; the same for the big cluster considered as a cluster of L_c small clusters, in units of the original lattice, is $\overline{K_c}=(1/L)(2\pi p/L_c)$, $p=0,\ldots,L_c-1$. Hence the reciprocal lattice points of the big cluster considered as a cluster of LL_c points are $K_c+\overline{K_c}$. We solve the DCA in real space with the big cluster of size LL_c:

$$G_{\alpha A,\beta B}(\omega)=\sum_{\overline{K}}\ \frac{1}{\omega-t^{\mathrm{cyc}}_{(\alpha,A),(\beta,B)}(\overline{K})-\Sigma_{\alpha A,\beta B}(\omega)}, \tag{A3}$$

$$t^{\mathrm{cyc}}_{(\alpha,A),(\beta,B)}(\overline{K})=\frac{1}{(LL_c)^d}\sum_{K_c,\overline{K_c}} e^{i(K_c+\overline{K_c})(\alpha+A-\beta-B)} \times t(\overline{K}+K_c+\overline{K_c}) \tag{A4}$$

$$=\frac{1}{L_c^d}\sum_{\overline{K_c}} e^{i\overline{K_c}(\alpha+A-\beta-B)}t^{\mathrm{cyc}}_{\alpha\beta}(\overline{K}+\overline{K_c}), \tag{A5}$$

where we used $K_cA=0\ [2\pi]$ in the last equation. Because of the reduced invariance, we can diagonalize using $\overline{K_c}$ and obtain

$$G_{\alpha\beta}(\overline{K_c},\omega) =\sum_{\overline{K}}\ \frac{1}{\omega-t^{\mathrm{cyc}}_{\alpha,\beta}(\overline{K}+\overline{K_c})e^{iK_c(\alpha-\beta)}-\Sigma_{\alpha,\beta}(\overline{K_c},\omega)}.$$

Using the *unitary* transformation,

$$\tilde{G}_{\alpha\beta}(\overline{K_c},\omega)\equiv e^{-i\overline{K_c}(\alpha-\beta)}G_{\alpha\beta}(\overline{K_c},\omega),$$

we obtain

$$\tilde{G}_{\alpha\beta}(\overline{K_c},\omega)=\sum_{\overline{K}}\ \frac{1}{\omega-t^{\mathrm{cyc}}_{\alpha,\beta}(\overline{K}+\overline{K_c})-\tilde{\Sigma}_{\alpha,\beta}(\overline{K_c},\omega)}. \tag{A6}$$

Let us now concentrate on the AF order: $L=2$ and for simplicity in dimension 1. In this case, $K_c=0,\pi$. We will now show that Eq. (A6) is equivalent to the k-space formulation presented in Ref. 16 (denoted by a superscript M). In the AF phase, correlations appear between k and $k+\pi$ and the self-consistency condition reads

$$G^M(\overline{K_c},\omega)=\sum_{\overline{K}}\left[\begin{pmatrix}\omega-t(\overline{K}+\overline{K_c}) & 0\\ 0 & \omega-t(\overline{K}+\overline{K_c}+\pi)\end{pmatrix} -\Sigma^M(\overline{K_c},\omega)\right]^{-1}, \tag{A7}$$

where G^M and Σ^M are 2×2 matrices, which are nondiagonal in the AF phase:

$$G^M \equiv -\begin{pmatrix} \langle Tc_k c_k^\dagger\rangle & \langle Tc_k c_{k+\pi}^\dagger\rangle \\ \langle Tc_{k+\pi} c_k^\dagger\rangle & \langle Tc_{k+\pi} c_{k+\pi}^\dagger\rangle \end{pmatrix}.$$

Using the transformation[16]

$$c_{1K}=\frac{c_K+c_{K+\pi}}{\sqrt{2}}, \quad c_{2K}=\frac{c_K-c_{K+\pi}}{\sqrt{2}}$$

Eq. (A7) is equivalent to Eq. (A6). Therefore the two formulations of DCA are equivalent in the antiferromagnetic phase.

The real-space formulation of DCA shares with CDMFT a property which is useful in practice: one does not have to *anticipate* the appearance of an ordered phase, i.e., to adapt the cluster scheme for the order to be described. The order will show up automatically solving the real-space DCA equations. Moreover, it can be more complex than an AF order, as long as the cluster is big enough to contain at least one unit cell.

APPENDIX B: LARGE-U LIMIT OF THE EFFECTIVE ACTION [PROOF OF EQS. (36)]

Here, we present some details of the derivation of the large-U limit of Eq. (26), in the limit where $U\to\infty$ with $\beta\to\infty$, β/U fixed. The effective action is

$$S_{\rm eff}=-\int\int_0^\beta d\tau d\tau' c_{\mu\uparrow}^\dagger(\tau)G_{0,\mu\nu\uparrow}^{-1}(\tau,\tau')c_{\nu\uparrow}(\tau')+\int_0^\beta d\tau \times c_{\mu\downarrow}^\dagger(\tau)\partial_\tau c_{\mu\downarrow}(\tau)+U\left(n_{\mu\uparrow}(\tau)-\frac{1}{2}\right)\left(n_{\mu\downarrow}(\tau)-\frac{1}{2}\right), \tag{B1}$$

$$G_{0\mu\nu\uparrow}^{-1}(i\omega_n)=i\frac{xU}{2}\delta_{\mu\nu}-\tilde{t}_{\mu\nu}(x)-\frac{2t}{U}J_\rho^{\mu\nu}(x)\langle h_\rho\rangle+O\left(\frac{1}{U^2}\right). \tag{B2}$$

We are going to compute the expression of partial partition function $Z[\{n_{\rho\downarrow}\}]$ (also denoted as $Z[\{S_\rho\}]$) as a function of the spins and recover Eqs. (36). We first compute the expansion of $\ln Z[\{n_{\rho\downarrow}\}]$ at second order in t and first order in J. We obtain

$$\ln(Z[\{S_\rho\}]/Z_0[\{S_\rho\}]) = \sum_{(i,j)}\sum_{i\omega_n,i\omega_n'}\tilde{t}_{ij}(i\omega_n)\tilde{t}_{ji}(i\omega_n') \times\langle c_{i\uparrow}^\dagger(i\omega_n)c_{j\uparrow}(i\omega_n)c_{j\uparrow}^\dagger(i\omega_n')c_{i\uparrow}(i\omega_n')\rangle_S + 2\sum_i\sum_{i\omega_n}J_\rho^{ii}(x)\langle h_\rho\rangle\langle c_{i\uparrow}^\dagger(i\omega_n)c_{i\uparrow}(i\omega_n)\rangle_S - O(t^3,J^2), \tag{B3}$$

where (i,j) denotes the sum over couples and $\langle\rangle_S$ is an average of the Gaussian action at fixed S. We see that

$$Z_0[\{S_\rho\}]\equiv Z_{t=J=0}[\{S_\rho\}]\propto\prod_\rho\cosh\left(\frac{\beta U}{4}S_\rho\right) \tag{B4}$$

is independent of S_ρ (since $S_\rho=\pm1$) and therefore it will be dropped in the following. Using the relations

$$\langle c_\rho(i\omega_n)c_{\rho'}^\dagger(i\omega_n')\rangle=-G_{\rho\rho'}^S(i\omega_n)\delta_{\omega_n,\omega_n'}, \tag{B5a}$$

$$G_{\rho\rho'}^S(i\omega_n)\equiv\frac{\delta_{\rho\rho'}}{i\omega_n+\frac{U}{2}S_\rho}=\frac{\delta_{\rho\rho'}}{2}\left(\frac{1-S_\rho}{i\omega_n-\frac{U}{2}}+\frac{1+S_\rho}{i\omega_n+\frac{U}{2}}\right) \tag{B5b}$$

and the fact that in the AF phase $\tilde{t}(-z)=\tilde{t}(z)$ since $\langle S_i\rangle+\langle S_j\rangle=0$, we can reduce the expression (B3), extract the S_iS_j term, and obtain finally

$$\ln(Z[\{S_\rho\}])=-\beta H_{\rm eff}+O(t^3,J^2) \tag{B6}$$

with $H_{\rm eff}$ given by Eqs. (36). The additional term $J_\rho^{\mu\nu}$ does not contribute to the $J_{\rm Ising}$ since it would give a $O(1/U^2)$ contribution. Moreover, since $J_{\rm Ising}\sim\tilde{t}^2/U$ we do not need to compute the $1/U$ term of $\Sigma^{\rm C}$.

Finally, higher orders in the expansion do not contribute. Indeed, since $Z[\{S_\rho\}]$ is a *Gaussian* action and since we compute $\ln Z[\{S_\rho\}]/Z_0$, we only get *connected diagrams*, thus we have one sum over Matsubara frequencies. Each Matsubara sum gives a factor βU [in the large-U limit Σ_{ω_n} is replaced by $\beta/4\pi\int d(xU)$] and each G a factor U^{-1}. Therefore higher-order terms are subdominant.

APPENDIX C: CLASSICAL LIMIT OF PCDMFT

In this appendix, we present the solution of Eqs. (9), (29), and (33) for completeness. We restrict ourselves to nearest-neighbor hopping. We start by solving at order 1 in the $1/U$ expansion. From Eqs. (29) and (33), we have for $\mu\neq\nu$ ($\Delta_{\mu\mu}=0$),

$$\Delta_{\mu\nu}^\alpha=t_{\nu-\mu}+\overline{\delta\Sigma^{{\rm latt}\alpha}_{\mu\nu}}-\Delta_{\mu\nu}^\alpha\frac{\langle h_\mu^\alpha h_\nu^\alpha\rangle_c}{\langle h_\mu^\alpha\rangle\langle h_\nu^\alpha\rangle}, \tag{C1}$$

where $\alpha=1,2$ is an index for the two (AF) solutions as in Eq. (9). Dividing the cluster into its two sublattices A and B with $\mathcal{C}=\mathcal{C}_A\cup\mathcal{C}_B$ and using Eq. (9), we have (for all $\mu\in\mathcal{C}$)

$$\overline{\delta\Sigma^{{\rm latt}\alpha}_{\mu,\mu+\delta}}=\frac{1}{S_c}\sum_{\substack{\rho\in\mathcal{C}_A\\ \rho+\delta\in\mathcal{C}}}\delta\Sigma^{{\rm C}\beta}_{\rho,\rho+\delta}+\frac{1}{S_c}\sum_{\substack{\rho\in\mathcal{C}_B\\ \rho+\delta\in\mathcal{C}}}\delta\Sigma^{{\rm C}\bar{\beta}}_{\rho,\rho+\delta}, \tag{C2}$$

where $\beta=\alpha$ if $\mu\in\mathcal{C}_A$, $\beta=\bar{\alpha}$ otherwise, since if $\rho+\delta\notin\mathcal{C}$, the exponential depends on K and averages to zero. For $\mu,\mu+\delta\in\mathcal{C}$, Eq. (C1) leads to

$$\Delta_{\mu,\mu+\delta}^\alpha\frac{\langle h_\mu^\alpha h_{\mu+\delta}^\alpha\rangle}{\langle h_\mu^\alpha\rangle\langle h_{\mu+\delta}^\alpha\rangle}=t_\delta+\frac{1}{S_c}\sum_{\substack{\rho\in\mathcal{C}_A\\ \rho+\delta\in\mathcal{C}}}\Delta_{\rho,\rho+\delta}^\beta\frac{\langle h_\rho^\beta h_{\rho+\delta}^\beta\rangle_c}{\langle h_\rho^\beta\rangle\langle h_{\rho+\delta}^\beta\rangle}+\frac{1}{S_c}\sum_{\substack{\rho\in\mathcal{C}_B\\ \rho+\delta\in\mathcal{C}}}\Delta_{\rho,\rho+\delta}^{\bar{\beta}}\frac{\langle h_\rho^{\bar{\beta}} h_{\rho+\delta}^{\bar{\beta}}\rangle_c}{\langle h_\rho^{\bar{\beta}}\rangle\langle h_{\rho+\delta}^{\bar{\beta}}\rangle}, \tag{C3}$$

for all μ,δ. The left-hand side depends only on whether $\mu \in \mathcal{C}_A$ or not. Therefore, for all δ, we can define for $\mu \in \mathcal{C}_A$ and $\zeta \in \mathcal{C}_B$,

$$F_\delta^{\alpha A} \equiv \Delta^\alpha_{\mu,\mu+\delta} \frac{\langle h^\alpha_\mu h^\alpha_{\mu+\delta}\rangle}{\langle h^\alpha_\mu\rangle\langle h^\alpha_{\mu+\delta}\rangle}, \tag{C4a}$$

$$F_\delta^{\alpha B} \equiv \Delta^\alpha_{\zeta,\zeta+\delta} \frac{\langle h^\alpha_\zeta h^\alpha_{\zeta+\delta}\rangle}{\langle h^\alpha_\zeta\rangle\langle h^\alpha_{\zeta+\delta}\rangle} \tag{C4b}$$

(they are independent of μ and ζ). Equation (C3) then leads to

$$F_\delta^{\alpha A} = t_\delta + A_{\delta\alpha} F_\delta^{\alpha A} + B_{\delta\alpha} F_\delta^{\bar{\alpha} B}, \tag{C5a}$$

$$F_\delta^{\alpha B} = t_\delta + A_{\delta\alpha} F_\delta^{\bar{\alpha} A} + B_{\delta\alpha} F_\delta^{\alpha B}, \tag{C5b}$$

$$A_{\delta\alpha} \equiv \frac{1}{S_c} \sum_{\substack{\rho\in\mathcal{C}_A \\ \rho+\delta\in\mathcal{C}}} \frac{\langle h^\alpha_\rho h^\alpha_{\rho+\delta}\rangle_c}{\langle h^\alpha_\rho h^\alpha_{\rho+\delta}\rangle},$$

$$B_{\delta\alpha} \equiv \frac{1}{S_c} \sum_{\substack{\rho\in\mathcal{C}_B \\ \rho+\delta\in\mathcal{C}}} \frac{\langle h^{\bar{\alpha}}_\rho h^{\bar{\alpha}}_{\rho+\delta}\rangle_c}{\langle h^\alpha_\rho h^\alpha_{\rho+\delta}\rangle}, \tag{C5c}$$

which can be rewritten as

$$(1-A_{\delta\alpha}) F_\delta^{\alpha A} - B_{\delta\alpha} F_\delta^{\bar{\alpha} B} = t_\delta, \tag{C6a}$$

$$(1-B_{\delta\alpha}) F_\delta^{\bar{\alpha} B} - A_{\delta\alpha} F_\delta^{\alpha A} = t_\delta. \tag{C6b}$$

The determinant of the equations for F is given by $\Pi_\alpha(1 - A_{\delta\alpha} - B_{\delta\alpha})$, which does not vanish for a generic x. For $|\delta|>1$, $t_\delta = 0$ by assumption hence $F_\delta^{\alpha A/B} = 0$. In the classical limit, the two solutions are related by a spin flip, so $\langle h^\alpha_\mu h^\alpha_\nu\rangle_c / \langle h^\alpha_\mu h^\alpha_\nu\rangle$ does not depend on α for μ,ν nearest neighbor, according to Eq. (31). For $|\delta| = 1$, the unique solution is obtained for equal $F_\delta \equiv F_\delta^{\alpha A/B}$, which is given by

$$F_\delta = \frac{t_\delta}{1 - \frac{1}{S_c} \sum_{\substack{\rho\in\mathcal{C} \\ \rho+\delta\in\mathcal{C}}} \frac{\langle h_\rho h_{\rho+\delta}\rangle_c}{\langle h_\rho h_{\rho+\delta}\rangle}}. \tag{C7}$$

Using the square symmetry, one can pick up one δ to compute the denominator. Hence, we obtain Eqs. (41a) and (41c) (the hopping is nearest neighbor). Note that the hopping is renormalized at order 1 (in $1/U$), but it is still restricted to nearest neighbors. In order to compute the J term, we now focus on $t + \delta\Sigma^{\text{latt}}$, which satisfies

$$\overline{(t+\delta\Sigma^{\text{latt}})}_{\mu,\mu+\delta} = F_\delta. \tag{C8}$$

It is a translation invariant quantity, which is also restricted to nearest neighbors. It has a formula analogous to Eq. (A1) for the hopping, and its value inside the cluster is given by its K average. Using Eq. (33c) to compute the mean-field terms $J^{\mu\mu}_\nu$, we see that the computation is similar than for CDMFT, with just a renormalization of the hopping (note, however, that $t + \delta\Sigma^{\text{latt}}$ is *not* the effective hopping $\tilde{t}$ defined as the order 1 term of Δ). In particular, the J_B terms have the same range as the original lattice hopping. Reporting Eq. (C8) into Eq. (33c) leads to Eq. (40a), which completes the derivation.

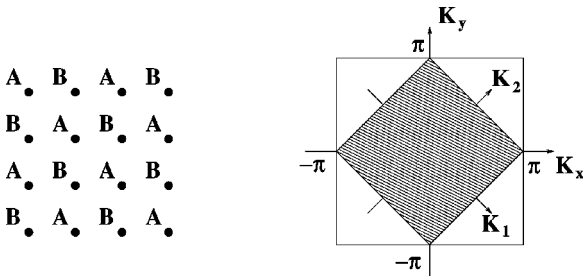

FIG. 4. Notations and reduced Brillouin zone for the pair scheme (shaded area).

APPENDIX D: CLASSICAL LIMIT OF THE PAIR SCHEME

The first task is to generalize the pair scheme in the presence of antiferromagnetic order. Denoting the two sublattices by A and B, we have the approximation for Φ,

$$\Phi_{pair} = (1-z)\left(\sum_{i\in A} \Phi_1[G_{ii}] + \sum_{j\in B} \Phi_1[G_{jj}]\right) + \sum_{\substack{\langle ij\rangle \\ i\in A \\ j\in B}} \Phi_2[G_{ii}, G_{jj}, G_{ij}]. \tag{D1}$$

We denote by (1) and (2) the one-site and the two-site model, respectively. We group the two one-site models into 2×2 diagonal matrices, and denote with an index *diag* the diagonal part of a matrix. To write the self-consistency condition, we take as unit cell one site on A, one site on B. K is now a vector in the corresponding reduced Brillouin zone, presented in Fig. 4. The hopping and the lattice self-energy are given by

$$t_{AA}(K) = t_{BB}(K) = 0, \tag{D2a}$$

$$t_{AB}(K) = tC(K), \tag{D2b}$$

$$C(K) = 1 + e^{-i(K_1-K_2)} + e^{i(K_1-K_2)} + e^{-i(K_1+K_2)}, \tag{D2c}$$

$$\Sigma^{\text{latt}}_{\text{diag}}(K) = \Sigma^{loc} = (1-z)\Sigma^{(1)}_{\text{diag}} + z\Sigma^{(2)}_{\text{diag}}, \tag{D2d}$$

$$\Sigma^{\text{latt}}_{AB}(K) = \Sigma^{(2)}_{12} C(K) \tag{D2e}$$

and the Green function by the usual formula (with 2×2 matrices)

$$G = \overline{[i\omega_n - t(K) - \Sigma^{\text{latt}}(K, i\omega_n)]^{-1}}.$$

The scheme implies consistency equations for the Green functions:

$$G^{(2)}=G, \quad G^{(1)}=D(G),$$

where we denote by D the linear operator that restricts a matrix to its diagonal.

First $G_{0\downarrow}$ is diagonal (with same proof as for the other schemes) but here it is not trivial:

$$\begin{aligned}(G_{0\downarrow}^{(1)})^{-1}(i\omega_n)&=i\omega_n+\Sigma_{\downarrow}^{(1)}(i\omega_n)-\Sigma_{\downarrow}^{\text{latt}}(i\omega_n)\\&=i\omega_n-z[\Sigma_{\downarrow}^{(2)}(i\omega_n)-\Sigma_{\downarrow}^{(1)}(i\omega_n)],\end{aligned} \tag{D3}$$

$$\begin{aligned}(G_{0\downarrow}^{(2)})^{-1}(i\omega_n)&=i\omega_n+\Sigma_{\downarrow}^{(2)}(i\omega_n)-\Sigma_{\downarrow}^{\text{latt}}(i\omega_n)\\&=i\omega_n-(z-1)[\Sigma_{\downarrow}^{(2)}(i\omega_n)-\Sigma_{\downarrow}^{(1)}(i\omega_n)].\end{aligned} \tag{D4}$$

Using previous notations, we have

$$\frac{\Delta_{\downarrow}^{(1)}(x)}{\Delta_{\downarrow}^{(2)}(x)}=\frac{z}{z-1}. \tag{D5}$$

Let us turn now to the up electrons. Introducing the notations

$$\overline{A}^{(2)}=\overline{A}, \quad \overline{A}^{(1)}=\overline{D(A)}$$

and, using that, for d a diagonal matrix independent of K, $\overline{Ad}^{(\alpha)}=\overline{A}^{(\alpha)}d$ (for $\alpha=1,2$), we can expand the self-consistency conditions

$$(G_0^{(1)})^{-1}=(G^{(1)})^{-1}+\Sigma^{(1)}, \tag{D6}$$

$$(G_0^{(2)})^{-1}=(G^{(2)})^{-1}+\Sigma^{(2)} \tag{D7}$$

with the expansion (33), to get

$$\Delta_{ii}^{(\alpha)}(x)=\overline{t}_{ii}^{(\alpha)}+\Sigma_{ii}^{loc}-\Sigma_{ii}^{(\alpha)}+\frac{2t}{U}J_{ii\rho}^{(\alpha)}(x)\langle h_{\rho}^{(\alpha)}\rangle + O\left(\frac{1}{U^2}\right) \quad (\alpha,i=1,2), \tag{D8a}$$

$$J_{\mu\nu\rho}^{(\alpha)}(x)\equiv\frac{1}{t}(\overline{\tilde{t}_{\mu\rho}\tilde{t}_{\rho\nu}}^{(\alpha)}-\overline{\tilde{t}_{\mu\rho}}^{(\alpha)}\,\overline{\tilde{t}_{\rho\nu}}^{(\alpha)}, \tag{D8b}$$

$$\tilde{t}(K,x)\equiv t(K)+\Sigma^{\text{latt}}(K,x). \tag{D8c}$$

Clearly, $\rho=\overline{i}$ with the notation $\overline{2}=1,\overline{1}=2$. Moreover,

$$\overline{\Sigma^{\text{latt}}}_{\text{diag}}^{(1)}-\Sigma^{(1)}=z(\Sigma_{\text{diag}}^{(2)}-\Sigma^{(1)}), \tag{D9a}$$

$$\overline{\Sigma^{\text{latt}}}_{\text{diag}}^{(2)}-\Sigma^{(2)}=(z-1)(\Sigma_{\text{diag}}^{(2)}-\Sigma^{(1)}) \tag{D9b}$$

and the J terms are given by

$$J^{(1)}=\frac{1}{t}\sum_{R}\tilde{t}_{\mu\rho}(R)\tilde{t}_{\rho\nu}(-R), \tag{D10a}$$

$$J^{(2)}=\frac{1}{t}\sum_{R\neq 0}\tilde{t}_{\mu\rho}(R)\tilde{t}_{\rho\nu}(-R), \tag{D10b}$$

which implies

$$J^{(1)}=zJ_0, \tag{D11a}$$

$$J^{(2)}=(z-1)J_0. \tag{D11b}$$

Therefore the equations for Δ simplify into

$$\Delta_{\uparrow ii}^{(1)}=z(\Sigma_{\text{diag}}^{(2)}-\Sigma^{(1)})+2zJ_0\langle h_i^{(1)}\rangle, \tag{D12a}$$

$$\Delta_{\uparrow ii}^{(2)}=(z-1)(\Sigma_{\text{diag}}^{(2)}-\Sigma^{(1)})+2(z-1)J_0\langle h_i^{(2)}\rangle. \tag{D12b}$$

Using that $m^{(1)}=m^{(2)}$, we have $\langle h_i^{(2)}\rangle=\langle h_i^{(1)}\rangle$ at dominant order and therefore

$$\frac{\Delta_{\uparrow ii}^{(2)}}{\Delta_{\uparrow ii}^{(1)}}=\frac{z-1}{z}. \tag{D13}$$

From Eqs. (D5) and (D13), using the computation of the classical field from Δ presented in Appendix B, we obtain the classical variation method defined in Eqs. (41) and (42).

Strictly speaking, we only prove here that, in the large-U limit, if there is a magnetic solution, it obeys the CVM equations. We have not shown that such nonzero solution exists. *A priori*, one could wish to push the semiclassical computation further and *compute* the classical field explicitly to check that it gives the values prescribed by the consistency of the classical equations. However, this is much harder to do than in previous schemes for the following reason. Contrary to all other schemes studied in this paper, there is no cancellation between the diagonal part of Σ^{latt} and of Σ^{C}. Therefore, we have to compute correction to $\langle h\rangle$ to order $1/U^2$, in order to compute Δ to order $1/U$ [the relation (31a) is *a priori* valid only at dominant order]. Because $\beta\sim U$, we need Δ up to order $1/U^3$ to get such a correction (like we need Δ at order $1/U$ to get a classical field of order 1). All these difficulties are hidden in the $\Sigma_{\text{diag}}^{(2)}-\Sigma^{(1)}$ term in Eq. (D12).

APPENDIX E: PROOF OF THE CUTKOVSKY-t'HOOFT-VELTMAN EQUATION

In this appendix, we prove the Cutkovsky-t'Hooft-Veltman formula using the Keldysh method.[24] We first briefly present our conventions.

1. Notations

We denote with a "+" the upper contour (going from $-\infty$ to ∞) and a "−" the lower contour. The definition of the Keldysh propagators (for fermions) is

$$-i\langle T\phi(x,t)\phi^{\dagger}(x',t')\rangle=G^{++}(x,x',t-t'), \tag{E1}$$

$$-i\langle \tilde{T}\phi(x,t)\phi^{\dagger}(x',t')\rangle=G^{--}(x,x',t-t'), \tag{E2}$$

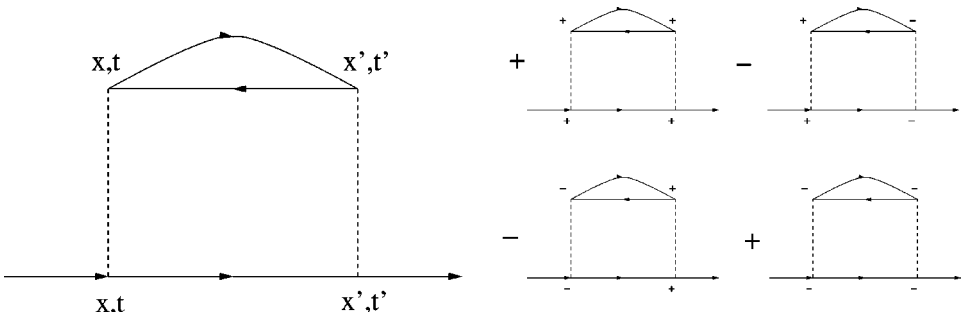

FIG. 5. A self-energy diagram and its Keldysh counterparts, with the Keldysh indices and the overall factor.

$$i\langle \phi^{\dagger}(x',t')\phi(x,t)\rangle = G^{+-}(x,x',t-t'), \tag{E3}$$

$$-i\langle \phi(x,t)\phi^{\dagger}(x',t')\rangle = G^{-+}(x,x',t-t'). \tag{E4}$$

After Fourier transformation $[\hat{f}(\omega)=\int dt e^{i\omega t} f(t)]$, we have, in particular, the following useful relations:

$$\rho(x,x',\omega) = -\frac{1}{\pi}\mathrm{Im}\, G_R(x,x',\omega), \tag{E5a}$$

$$G^{+-}(x,x',\omega) = 2i\pi\rho(x,x',\omega)\,\theta(-\omega), \tag{E5b}$$

$$G^{-+}(x,x',\omega) = -2i\pi\rho(x,x',\omega)\,\theta(\omega), \tag{E5c}$$

$$[G^{++}(x,x',\omega)]^{*} = -G^{--}(x',x,\omega). \tag{E5d}$$

To illustrate the diagrammatics, consider, for example, a second-order self-energy diagram in Fig. 5. It corresponds to

$$G_{x,x',t-t'}G_{x,x',t-t'}G_{x',x,t'-t}.$$

The Keldysh counterparts of the diagram are obtained by replacing each vertex by his corresponding Keldysh counterpart (see Fig. 5). They correspond to

$$\begin{aligned} &G^{++}_{x,x',t-t'}G^{++}_{x,x',t-t'}G^{++}_{x',x,t'-t} - G^{+-}_{x,x',t-t'}G^{+-}_{x,x',t-t'}G^{+-}_{x',x,t'-t} \\ &\quad - G^{-+}_{x,x',t-t'}G^{-+}_{x,x',t-t'}G^{-+}_{x',x,t'-t} \\ &\quad + G^{--}_{x,x',t-t'}G^{--}_{x,x',t-t'}G^{--}_{x',x,t'-t}, \end{aligned}$$

where $G^{\pm,\pm}$ are the Keldysh propagators.

2. Proof

The first point is to write the imaginary part of the zero-temperature retarded self-energy in terms of the Keldysh components:

$$\mathrm{Im}\,\Sigma_R(\omega) = \frac{\Sigma_{+-}(\omega)-\Sigma_{-+}(\omega)}{2i}. \tag{E6}$$

An important point is that this relation must hold for each diagram individually, in order to be compatible with any approximation considered as a diagram summation. Indeed at $T=0$ for $\omega>0$,

$$\Sigma_R(\omega) = \frac{1}{2i}[\Sigma_{++}(\omega)+\Sigma_{+-}(\omega)]$$

and using Eqs. (E5b) and (E5c), it is sufficient to prove that

$$\Sigma^{++}+\Sigma^{--}+\Sigma^{+-}+\Sigma^{-+}=0 \tag{E7}$$

is verified for each diagram individually. A way to prove that, which is actually in Veltman's book,[21] consists in noticing that each diagram with a "+" at the largest time vertex cancels against the same diagram with a "−" at this largest time vertex. This happens because $G^{++}(t-t')=G^{-+}(t-t')$ and $G^{--}(t-t')=G^{+-}(t-t')$ for $t>t'$ so the only thing that changes between one diagram and the other is a minus sign (associated with the "−" vertex and not with the "+" vertex). This is called by Veltman *the largest time equation*. To unveil this relationship we use the following notation: circle a vertex if it corresponds to ϕ^{-} and do not circle it if it corresponds to ϕ^{+}. Then the relationship with Veltman rules to obtain the largest time equation will become clear.

To obtain the Keldysh expansion of $\mathrm{Im}\,\Sigma_R$, we can thus take the expansion of Σ (as defined with any perturbation theory) and put Keldysh indices on it (as explained in the preceding section). First, we will focus on $\omega>0$. Then $\Sigma_{+-}(\omega)=0$, we only need to compute Σ_{-+}, i.e., the diagram with a "+" at the incoming vertex, and a "−" at the outgoing vertex. The crucial properties of zero-temperature diagrams are the following. Due to the presence of θ functions in frequency for G^{+-} and G^{-+} (cf. the preceding section), the frequency always flows from the "+" vertex to the "−" vertex. This implies that a diagram is zero if it contains a "−" vertex to which no external line is connected and that is surrounded by "+" vertices because of frequency conservation (the same is true if one replaces "+" with "−"). This cancellation generalizes to a connected set, or region, of "−" to which no external line is connected and that is surrounded by "+" vertices. Since we only have two external vertices, the nonvanishing diagrams are those with a line that cuts propagators, dividing them into a "+" region L on the left (connected to the incoming vertex) and a "−" region R on the right (connected to the outgoing vertex). This line is the cut of the diagram and the sum over Keldysh indices reduces to the sum over all possible cuts (see Fig. 1). In the L (R) region, we have to use G^{++} (G^{--}). Since $G^{--}(x,x',\omega)=-[G^{++}(x',x,\omega)]^{*}$, the R part gives D^{*}_{MR} times $(-1)^{\text{number of internal lines}}$, where MR is the (left) diagram part obtained from R by inverting all the arrows. Finally, to each cut line going from right to left (left to right) is associated a G^{+-} (G^{-+}) propagator. Hence we obtain the third rule of the text: each cut line going from left to right (right to left) is replaced by $\rho(x,x',\omega)\,\theta(\omega)$ $[\rho(x,x',\omega)\,\theta(-\omega)]$.

So there are two last things that remain to be clarified in order to get Eq. (44): (1) that the symmetry factors are taking into account correctly and (2) that the phase between the half left and right diagram is the one leading to Eq. (44). Concerning the symmetry factors, one has to be sure that all the counting is done correctly. In order to do this, it is useful to replace each half (or left) diagram with the sum of all half diagrams obtained from the original one permuting the cut lines in all the possible ways. The symmetry factor that one has to attach to them is exactly the one needed to get back the right symmetry factor for the original diagram by gluing together the half-right and the half-left diagrams. The ''gluing'' operations means attaching to each *i* line (see Fig. 2) of the half diagram the corresponding *i* line of the left diagrams. Indeed, to get the symmetry factor of a given diagram, one has to write all the topologically equivalent ways to obtain the same diagram. This can be done starting from the left and from the right, i.e., writing all the different ways to get the same topologically equivalent left and right diagrams and then attaching them in all the possible ways that give rise to the original diagram. Thus, the symmetry factors related to half or left diagrams are just all the different ways (contractions) that can be used to create them. In this way the operation of ''gluing'' together a half and left diagram in which all the cut lines have been permuted produces $n!$ (n is the number of cut lines) times the original uncut diagrams. The $1/n!$ in Eq. (47) is there exactly to balance this redundant $n!$ term.

Finally, let us focus on the phase between the right part of the diagram and D^*_{MR},

$$a=(-1)^{l_R}(-1)^{v_{\alpha R}}(-1)^{v_{\alpha R}(n_\alpha+1)}(-1)^{n_{loop}}(-i)^n(i)^{n-1}. \tag{E8}$$

The first term comes from the sign in $G^{--}=-G^{++*}$, with l_R the number of internal lines inside the right part R. The second term comes from the ''$-$'' Keldysh vertices, with $v_{\alpha R}$ the number of vertices of type α in the right part. The third term comes from the $(-i)^{n_\alpha+1}$ factor of each vertice at $T=0$ with n_α the number of outgoing lines in the vertices of type α: this factor changes under conjugation. The fourth term comes from the n_{loop} broken loops in the cut diagrams (we restrict ourselves for fermions here). The fifth and sixth terms come from the difference between G_{+-} and ρ (in the cut propagators going from left to right and right to left, respectively). The number of cut loops is given by $n_{loop}=n-1$. Moreover, summing all lines ending at a vertex in the right part, we have

$$\sum_\alpha v_{\alpha R} n_\alpha = l_R + n \quad [2], \tag{E9}$$

where $[2]$ is the reduction modulo 2. Finally we get $a=i$, which, combined with Eq. (E6), leads to Eq. (44). Similarly, for $\omega<0$, we have $\mathrm{Im}\,\Sigma_R=\Sigma_{+-}/2i$. The left part has ''$-$'' vertices, the right part ''$+$'' vertices. Using a similar analysis, we get $a=-i$, which leads to Eq. (44).

[1] A. Georges, G. Kotliar, W. Krauth, and M.J. Rozenberg, Rev. Mod. Phys. **68**, 13 (1996).

[2] S. Savrasov, G. Kotliar, and E. Abrahams, Nature (London) **410**, 793 (2001); S. Biermann, F. Aryasetiawan, and A. Georges, Phys. Rev. Lett. **90**, 086402 (2003).

[3] V. Dobrosavljevic and G. Kotliar, Phys. Rev. B **50**, 1430 (1994); Acta Phys. Pol. A **85**, 21 (1994).

[4] Q. Si and J.L. Smith, Phys. Rev. Lett. **77**, 3391 (1996); J.L. Smith and Q. Si, Phys. Rev. B **61**, 5184 (2000).

[5] A. Schiller and K. Ingersent, Phys. Rev. Lett. **75**, 113 (1995).

[6] G. Zarand, D. Cox, and A. Schiller, Phys. Rev. B **62**, 16227(R) (2000).

[7] T. Maier, M. Jarrell, T. Pruschke, and J. Keller, Eur. Phys. J. B **13**, 613 (2000); M.H. Hettler, A.N. Tahvildar-Zadeh, M. Jarrell, T. Pruschke, and H.R. Krishnamurthy, Phys. Rev. B **58**, 7475(R) (1998).

[8] G. Biroli and G. Kotliar, Phys. Rev. B **65**, 155112 (2002).

[9] G. Kotliar, S.Y. Savrasov, G. Pálsson, and G. Biroli, Phys. Rev. Lett. **87**, 186401 (2001).

[10] T.A. Maier and M. Jarrell, Phys. Rev. B **65**, 041104 (2002).

[11] C.J. Bolech, S.S. Kancharla, and G. Kotliar, Phys. Rev. B **67**, 075110 (2003).

[12] A. Lichtenstein (private communication).

[13] A.I. Lichtenstein and M.I. Katsnelson, Phys. Rev. B **62**, 9283(R) (2000).

[14] S. Pankov, G. Kotliar, and Y. Motome, Phys. Rev. B **66**, 045117 (2002).

[15] R. Mills and P. Ratanavararaksa, Phys. Rev. B **18**, 5291 (1978); R. Mills, T. Kaplan, and L.J. Gray, *ibid.* **27**, 3252 (1983).

[16] T.A. Maier, http://www.physics.uc.edu/~jarrell/thesis_tmaier.ps.gz

[17] R. Kikuchi, Phys. Rev. **81**, 988 (1951).

[18] T. Morita, J. Stat. Phys. **59**, 819 (1990).

[19] B.G. Nickel and W.H. Butler, Phys. Rev. Lett. **30**, 373 (1973).

[20] J.K. Freericks and V. Zlatic, cond-mat/0301188 (unpublished).

[21] M. Veltman, *Cambridge Lecture Notes in Physics* (Cambridge University Press, Cambridge, 1994).

[22] S. Okamoto, A.J. Millis, H. Monien, and A. Fuhrmann, Phys. Rev. B **68**, 195121 (2003).

[23] M. Capone and M. Civelli (unpublished).

[24] L.V. Keldysh, Zh. Eksp. Teor. Fiz. **47**, 1515 (1964) [Sov. Phys. JETP **20**, 1018 (1965)]; J. Rammer and H. Smith, Rev. Mod. Phys. **58**, 323 (1986).